ACTIVE SUSPENSION FOR THREE AXLE RAILWAY VEHICLE

MOHAMMAD SABERI BIN AHMAD

UNIVERSITI MALAYSIA PAHANG

ACTIVE SUSPENSION CONTROL OF THREE AXLE RAILWAY VEHICLE

MOHAMMAD SABERI BIN AHMAD

This thesis is submitted as partial fulfillment of the requirement for the Award of the Bachelor Degree of Electrical Engineering (control and instrumentation)

Faculty of Electrical & Electronic Engineering
University Malaysia Pahang

NOVEMBER 2009

DECLARATION

"All the trademark and copyrights use here in are property of their respective owner. References of information from other sources are quoted accordingly, otherwise the information presented in this report is solely work of the author".

Signature : ______________________________

Author : MOHAMMAD SABERI BIN AHMAD

Date :

DEDICATION

Specially dedicate to

My beloved parents, lecturers, brother and sisters.

ACKNOWLEDGEMENT

First and foremost, I am very grateful to the Allah throughout all His Almighty kindness and loveliness for giving me the key and opportunity to accomplish my Final Year Project.

In particular, I wish to express my sincere appreciation to my supervisor, Mister Anwar bin Zawawi for encouragement, guidance, suggestions, critics and friendship throughout finishing this project.

Secondly, I wish to thank all persons who have helped me directly or indirectly. I am very thankful to all my friends who gave me support and idea to finish this project, especially Mohd. Amir Izat b. Mhd Rodzi who always with me to settle any problem together.

Most importantly, I wish my gratitude to my parents for their support, encouragement, understanding, sacrifice and love. For all of that, I am very thankful to the cooperation and contribution from everyone that has driven me to accomplish of this project. There is no such meaningful word then…. May God bless all of you.

ABSTRACT

Nowadays, active suspension system is commonly used in many vehicles to overcome the limitation of passive suspension. This project will apply the active suspension system into the railway vehicles to study the performance of the train. This paper will focus for three axle railway vehicle. In term to study the three axle railway vehicle, there are four results that need to be observed. The four results that should be observed are control torque, lateral displacement, yaw angle, and body acceleration. We will use different value of parameter to see the parameter's characteristic that will contribute to better performance. The parameters that will be tested are cant angle, curving track radius and vehicle velocity. The system will be form in state space equation. From state space equation, three axle railway vehicles will be presented using MATLAB application. Linear quadratic regulator is used to be the controller in this project. Simulation on MATLAB application is analyzed.

ABSTRAK

Pada masa ini, sistem suspensi aktif selalu digunakan di dalam banyak jenis kenderaan untuk mengatasi kelemahan sistem suspensi pasif. Projek ini akan menggunakan sistem suspensi aktif kepada kenderaan jenis keretapi untuk mengkaji hasil prestasi keretapi tersebut. Projek ini akan memfokuskan kepada sistem keretapi bergandar tiga. Untuk mengkaji prestasi keretapi bergandar tiga ini, empat keputusan akan dilihat. Empat keputusan itu adalah kawalan 'torque', anjakan secara melintang (lateral) and rewang (yaw) serta pecutan untuk badan keretapi tersebut. Dalam projek ini, parameter yang berlainan akan digunakan untuk mengkaji kriteria yang terbaik yang menyumbang kepada prestasi keretapi yang baik. Parameter-parameter yang akan diuji tersebut adalah seperti sudut 'cant", jejari selekoh dan juga halaju keretapi tersebut. Sistem ini akan disusun di dalam bentuk rumus 'state-space". Daripada rumus 'state-space' tersebut, sistem ini akan ditunjukkan melalui aplikasi MATLAB. LQR akan digunakan sebagai pengawal di dalam projek ini. Keputusan simulasi di dalam aplikasi MATLAB akan dikaji.

TABLES OF CONTENTS

CHAPTER 1

INTRODUCTION

1.1 BACKGROUND

This project is based on modeling the active suspension for three axle railway vehicle and to study the controller design of LQR. The modeling of three axle railway vehicle will be done in state space equation and will be presented in MATLAB software. The goal of this project is to study about the train's performance which is determined from control torque, yaw angle, lateral displacement, and vehicle body acceleration result. In this project, the train's performance will be tested by using different value of parameter. The parameters values that will be changed are cant angle, curving track radius, and vehicle velocity. The parameters value will be tested to analyze the best characteristic of the parameter that will contribute to the train's higher performance.

In this project, controller LQR will be used. Linear Quadratic Regulator (LQR) controller are developed using mathematical equation to get the feedback for control torque, lateral displacement, yaw angle and body acceleration using MATLAB application. The LQR tuning algorithm in railway vehicle is applied to control the performance of three axle railway vehicles. The performance measure to be minimized contains output error signal and differential control energy. The LQR receives error signal only and it doesn't need to feedback full states. The Q matrix can be determined from the roots of the characteristics equation. Once the poles for the closed-loop system are assigned, the existence criteria of the LQR controller are derived.

1.2 DEPENDENT ROTATING WHEELSET

The most important component in a railway vehicle system is its wheelset. The wheelset consists of two coned (or otherwise profiled) shape wheels connected by an axle. In this project, the solid axle used is dependent rotating wheelset type. Both of the wheels are depends each other, meaning that the rotating wheels will be same in speed of rotation. So, when the train meet a curve track, the inner side of the wheels has a larger radius wheel flange compared to the outer side. Figure 1.2 shows the features of a railway solid-axle wheelset [1].

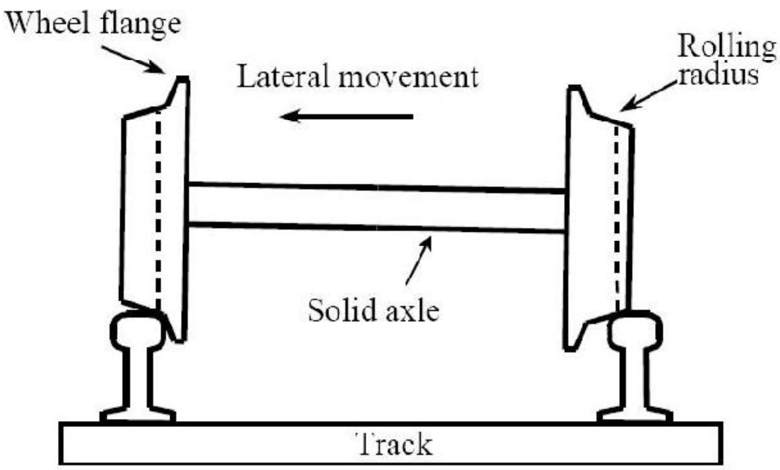

Figure 1.1: Solid-axle railway wheelset features.

1.3 WHEELSET DYNAMICS.

On straight track, the wheelset runs in a centralized position as shown in Figure 1.3(a). When the vehicle wheelset encounters a curve, it naturally moves outwards. The side by side wheels connected by an axle run on different radius at that moment. The outer wheel runs on a larger radius but the inner wheel moves with a smaller radius as can be seen in Figure 1.3(b). Both wheels have to rotate at the same rotational speed, thus the outer wheel moves faster along the track. In design purpose, it is important to make sure there is no contact between the wheel flange and the rail to avoid large amount of wear on the wheels and rails and to reduce noise [2].

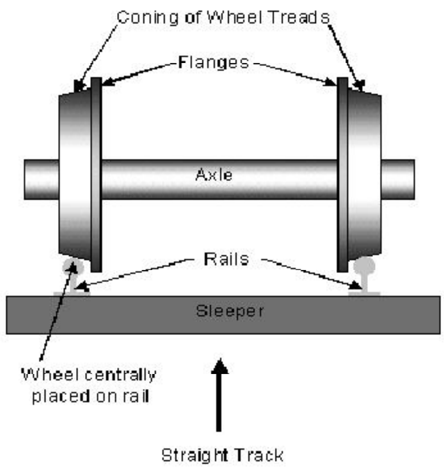

Figure 1.3(a): Wheelset on straight track

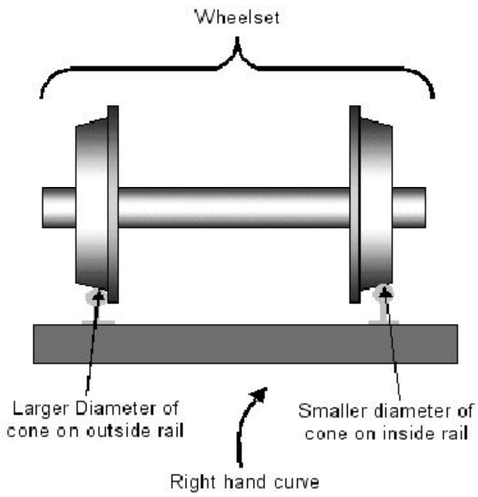

Figure 1.3(b): Wheelset on curve track

For a single wheelset, the second-order differential equations that represent the relationship of creep damping and creep stiffness coefficient with lateral and yaw displacement can been shown below [3]:

$$\ddot{y}=\frac{-2f_{11}}{mV}\dot{y}+\frac{-2f_{22}}{m}\psi+\frac{1}{m}F_y \quad (2.1)$$

$$\ddot{\psi}=\frac{-2f_{11}l\lambda}{I_w r}y-\frac{-2f_{11}l^2}{I_w V}\dot{\psi}+\frac{1}{I_w}T_w \quad (2.2)$$

where;

y is the lateral displacement of the wheelset
ψ is the yaw angle (angle of attack)
F_y is the external lateral force
T_ψ is the external yaw torque
m is the mass of the wheelset
I_w is the moment of inertia of the wheelset
f_{11} is the longitudinal creep coefficient of the wheelset
f_{22} is the lateral creep coefficient of the wheelset

1.4 PROBLEM STATEMENT

The active suspension is commonly used now to overcome the limitation of the passive suspension. The track input for the straight and curved track will be tested with different value of parameters (cant angle, curve radius, and vehicle's velocity) to see the best characteristic of each parameter to contribute for the best performance.

1.5 OBJECTIVE

The main core objective of the project is to establish the model of the active suspension for three axle railway vehicles system by using state space and to study the wheelset curving performance of railway vehicle by comparing the result of the train performance (control torque, lateral displacement, yaw angle and body acceleration).

1.6 SCOPES

In order to achieve this project, there are several scopes had been outlined:

i. Model railway vehicle with three sets of wheel set.
ii. Using actual parameter for railway vehicle. The parameters value are referred to the related paper.
iii. Track input – straight and curved track with curve radius and cant angle
iv. Using modern control system to control the performance.
v. Use MATLAB to simulate and analyze the system.

1.7 METHODOLOGY

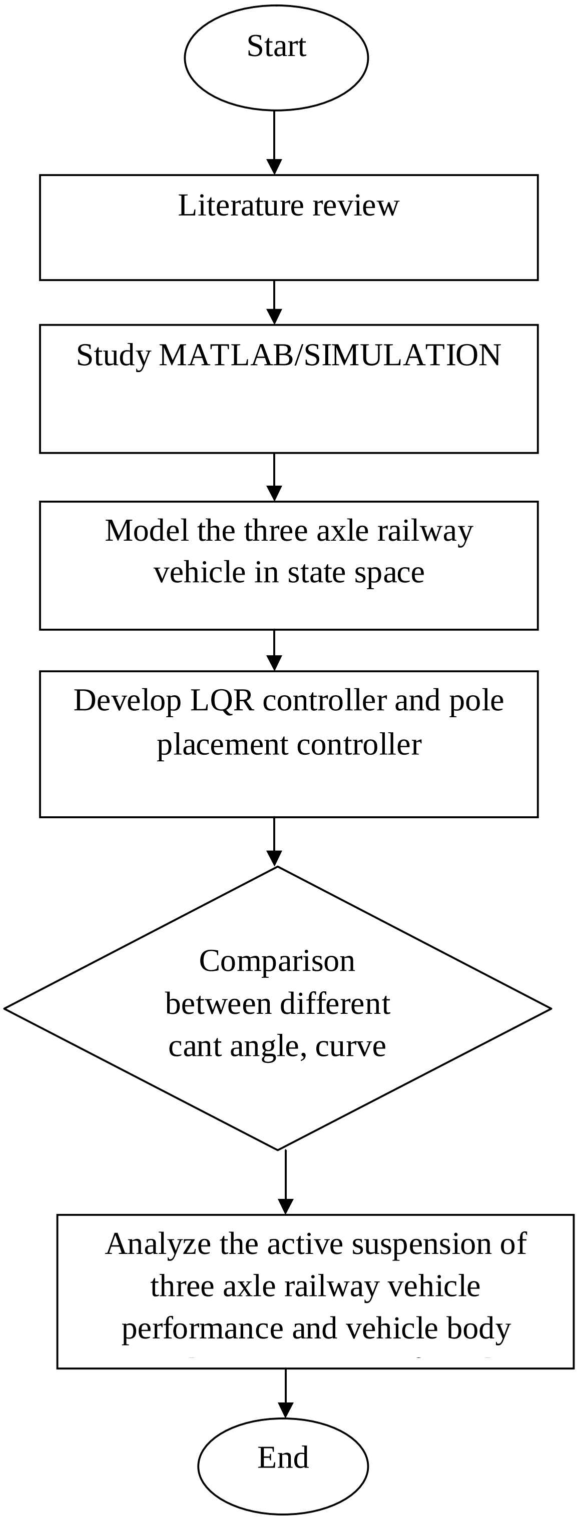

CHAPTER 2

LITERATURE REVIEW

2.1 INTRODUCTION

In this chapter include the study of active suspension system, three axle railway vehicle, and railway track profile. At the last of this chapter, the controller LQR will be discussed.

2.2 ACTIVE SUSPENSION

Active suspension is commonly used nowadays due to its ability to overcome the limitation of passive suspension. The active suspension consists of a controller, sensor and actuator compare to passive suspension that just consists of spring and damper. The sensor is functioning as to measure and sense the variable changes in the process. Then, the data will send to the controller and the controller will provide command to the actuator. The actuator will apply force or torque to the system to make the system more reliable [4].

Active suspension also requires for an external power source to achieve the desired suspension goal. The active suspension system provides the freedom to adjust the entire suspension system, and the control force can be introduced locally or globally based on the system state [5].

2.3 THREE AXLE RAILWAY VEHICLE

Active suspension for three axle railway vehicle is the improvement from the research of the active suspension for two axle railway vehicle. In this project, one more axle is added between the front wheelset and the rear wheelset to become the middle wheelset. The effect of the addition wheelset to the train's performance will be study.

The arrangement for three axle railway vehicle is shown in Figure 2.1. The system consists of the damper and spring which connect to the wheelset as the suspension element and addition of sensor and actuator connected from wheeset directly to the train's body to make it as the active element [6].

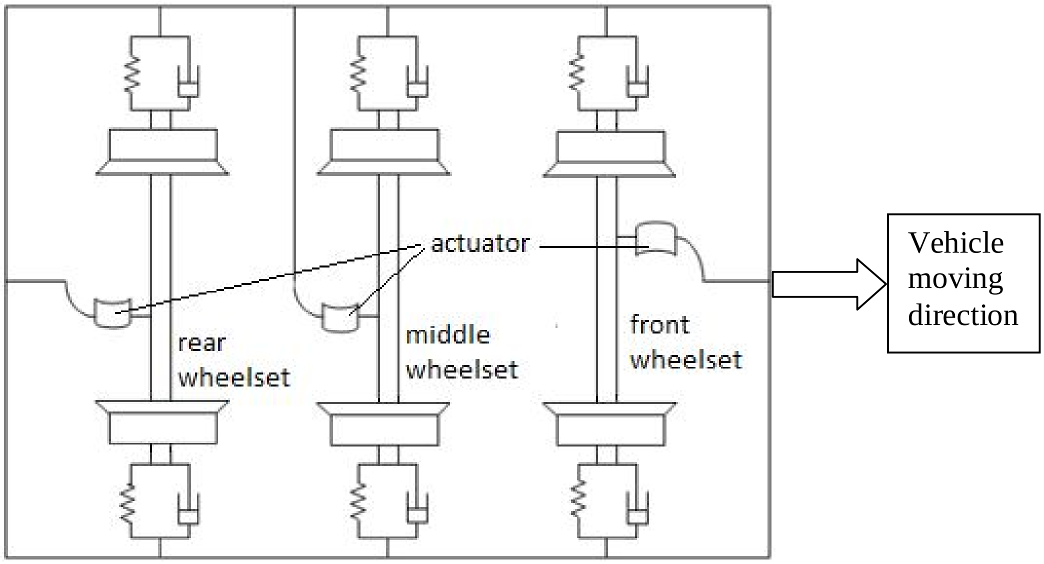

Figure 2.1: Three axle railway vehicle arrangement

2.4 RAILWAY TRACK PROFILE

2.4.1 CURVE RADIUS AND CANT ANGLE

To study the suspension curving performance, the input of the system has to be a curved track with a certain radius and corresponding cant angle (a deterministic track input). In this research, the curved track is connected to straight tracks on either end via one second time transition. The time transition is necessary to reduce the curving effects on the vehicle's passenger. The curved track is canted inwards to reduce the lateral acceleration experienced by the passengers [7]. The vehicle speed (e.g. balance speed) on curved track can be determined from the following balance equation:

$$V_{bal} = \sqrt{R \times g \times \tan\theta_c} \tag{2.3}$$

where;

V_{bal} is the balance speed (ms^{-1})
R is the curve radius (m)
g is the gravity (9.81 ms^{-2})
θ_c is the cant angle (deg.)

In this study, the curve radius is 1500 m and the cant angle is 14^o. This will give the balance speed at curved track equal to 60.6 ms^{-1}. As the vehicle is required to run at a higher speed level (e.g. 60 ms^{-1}), the cant deficiency standard has to be fulfilled for safety purposes.

2.4.2 CANT DEFIECIENCY

Cant is defined as the elevation of the outside rail minus the elevation of the inside rail of a curved track (synonym to the superelevation of the curve). Cant deficiency presents when a vehicle's speed on a curve is greater than the speed (e.g. *balance speed*) at which the components of wheel to rail force normal to the plane of the track would be the same in aggregate for the outside rails as for the inside rails. For a railway vehicle that travels at a higher speed than the balancing speed, the cant deficiency is given as follow:

$$CD = \frac{g_r}{\sqrt{1+\frac{R^2 g^2}{V^4}}} - SE \tag{2.4}$$

where;

CD is cant deficiency (mm)
g is the gravity
g_r is the rail gauge (mm)
R is the curve radius
SE is the superelevation of the track (mm)
V is the vehicle speed (ms^{-1})

According to the standard gauge railroads in the United States, the superelevation is limited to eight inches (8”) or equal to 203.2 mm [8]. As for the rail gauge, the standard value is 1435 mm [9]. The standard value for cant deficiency is different between countries, and it is depending on the type of the vehicle (tilting or non-tilting trains) [10]. In this study, the maximum allowable cant deficiency is referred to the United States standard for non-tilting trains which is seven inches (7”) or equal to 177.8 mm.

As the vehicle is required to travel at a speed level which is higher than the balance speed, the cant deficiency is calculated to make sure it is within the permitted value. The superelevation of the track is calculated from the selected cant angle and standard rail gauge values and give the superelevation value equal to 176.2 mm. Next, the cant deficiency can be found using Equation (2.4). For the selected parameter values of track profile in this study, the cant deficiency is 144.3 mm which is lower than 177.8 mm.

2.5 LINEAR QUADRATIC REGULATOR (LQR).

Linear quadratic regulator or LQR is commonly used technique to find the state feedback gain for a closed loop system. This is the optimal regulator, by which the open-loop poles can be relocated to get a stable system with optimal control and minimum cost for given weighting matrices of the cost function. On the other hand, by using the optimal regulator technique, that freedom of choice is lost for both discrete-time and continuous-time systems, because, in order to get a positive-definite Riccati equation solution, there are some areas where the poles cannot be assigned [11]

A crucial step in the LQR design process is the selection of the quadratic weighting matrices. These matrices determine the Kalman steady state gain and ultimately the state response [12]. Algorithms which aid in the selection of the quadratic weights based on some specified criteria are very desirable since they eliminate a trial and error weight selection process. The LQR problem can be solved for either the continuous or discrete time case. Each method yields an optimal gain. These gains are not interchangeable.

The problem presented by the infinite horizon LQR formulation is given a linear n-dimensional state variable system of the form: $\dot{x}(t) = Ax(t) + Bu(t)$ Compute the m-dimensional control input vector u(t), such that the performance index is minimized. Quadratic weighting matrices Q and R are selected by the designer to give appropriate state responses. It is well known that the solution is $u(t) = -Kx(t)$, where the

Kalman gain, ***K,*** is given by $K = R^{-1}B^{\mathrm{T}}P$,with ***P*** being the solution to the algebraic Riccati equation,$0 = A^{\mathrm{T}}P + PA - PBR^{-1}B^{\mathrm{T}}P + Q$.

The gain vector $K = R_{-1}B'P$ determines the amount of control fed back into the system. The matrix R and Q, will balance the relative importance of the control input and state in the cost function (J) being optimized with a condition that the elements in both Q and R matrices are positive values. The size of Q matrix depends on the size of the system's state matrix and R matrix is dependent on the number of control input to the system [13].

Using MATLAB, the algebraic Ricatti equation is solved and the control gain K is evaluated for different values of Q and R weighting matrices. The response of the system is simulated as well. The weighting matrix R is a scalar value as there is only one control input to the system. The values in the Q matrix are adjusted according to the required response of the system; a higher value of the weightings indicates the importance of the states [14].

CHAPTER 3

DYNAMIC MODELING

3.1 INTRODUCTION

In this chapter, the characteristics of a solid axle wheelset that should be considered will be discussed. Then the mathematical equation that will be form into state space equation will be explained.

3.2 SOLID AXLE WHEELSET CHARACTERISTICS

Nowadays, solid axle wheelset is commonly used due to it offers many advantages. Figure 3.1 and Figure 3.2 show two of the solid axle wheelset which are conical type and profiled type. This project chapter will discuss on solid axle wheelset characteristics which are about natural curving, perfect curving, wheelset hunting and mathematical description including state space representation [1].

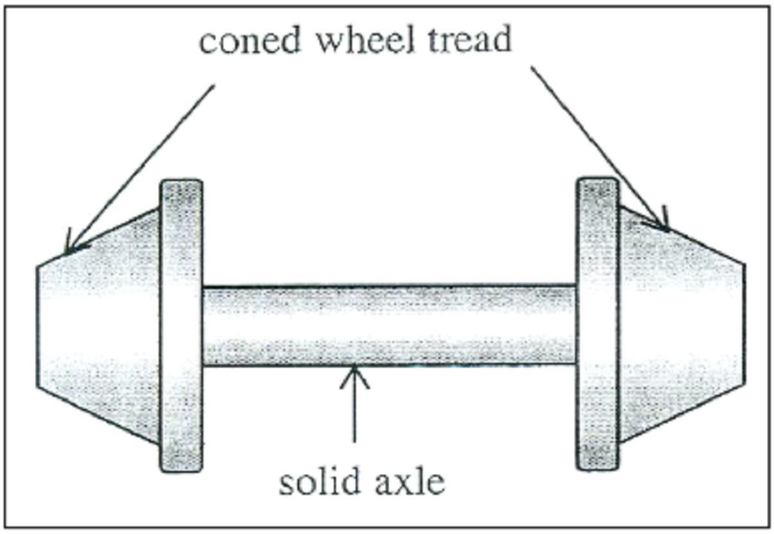

Figure 3.1: Conical Wheelset

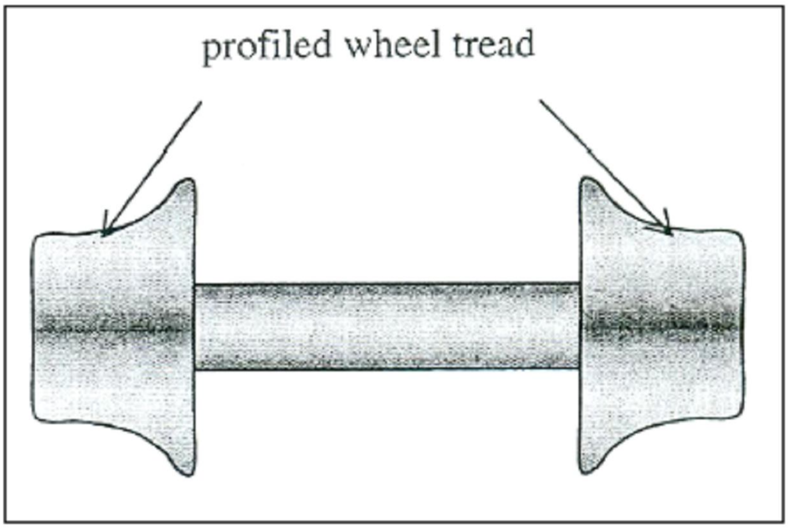

Figure 3.2: Profiled Wheelset

3.2.1 NATURAL CURVING

The important element for solid-axle wheelset is a pair of wheels which is coned or profilled tread. In this project, the dependent rotating wheelset will be used, so the wheels are rigidly connected to a common axle. The wheels must rotate at the same rotational speed, thus the outer wheel moves faster along the track, and the effect is to make the wheelset go around the curve. Some misconception is that, it is the flange which makes the vehicle follows the curve. But in fact, it is entirely a result of the profiling of the wheels. This advantage of following the rail track particularly on curved track is also known as 'natural curving' [1].

3.2.2 PERFECT CURVING

When the railway vehicle moves along a curved track, the wheelsets tend to move inside of the curve radius laterally besides experiencing the cant angle displacement at the same time. To achieve a pure rolling action (the perfect curving), it is necessary to choose a good control scheme to enhance the curving performance of the vehicle suspension system [1].

3.2.3 WHEELSET HUNTING

Because the wheels are connected together to a common axle, this wheelset is also inherently unstable at any non-zero speed and it exhibits a sustained oscillation in the lateral plane or known as 'wheelset hunting'. Figure 3.3 shows the wheelset moves in sinusoidal direction due to the characteristics of the wheelset [1].

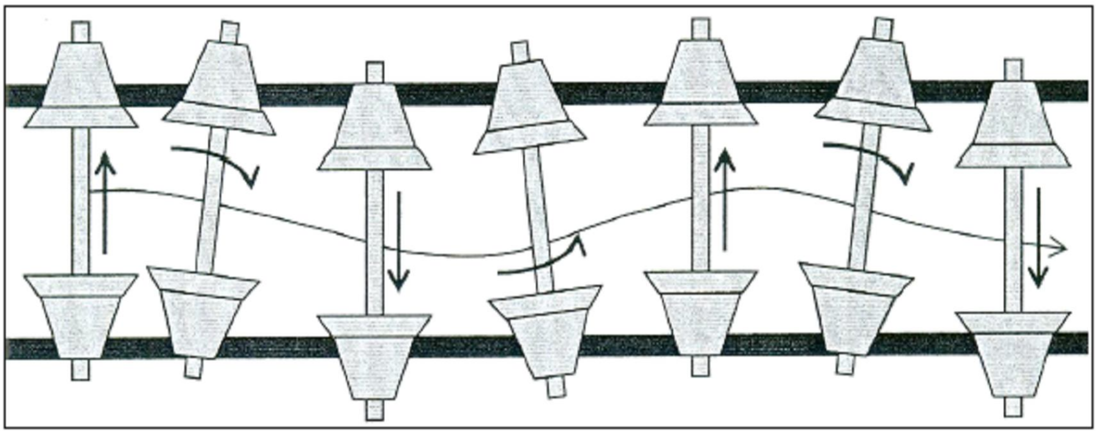

Figure 3.3: Wheelset Hunting

3.2.4 MATHEMATICAL DESCRIPTION

The complete equations of linear model of a single solid axle wheelset travelling on a straight track with lateral irregularities are given in Equations (3.1) and (3.2) below [15]:

$$m\ddot{y}_w = \frac{-2f_{22}}{V}\dot{y}_w + 2f_{22}\psi_w + F_y \tag{3.1}$$

$$I_w\ddot{\psi}_w = \frac{-2f_{11}l\lambda}{r}y_w - \frac{-2f_{11}l^2}{V}\dot{\psi}_w + T_\psi \tag{3.2}$$

3.2.5 STATE-SPACE REPRESENTATION

The differential equations in equations (3.1) and (3.2) are represented in state space form as below:

$$\dot{x} = A_w x + B_w u \tag{3.3.1}$$

$$y = C_w x + D_w u \tag{3.3.2}$$

where;

$$x = [\begin{array}{cccc} x_1 & x_2 & x_3 & x_4 \end{array}]^T = [\begin{array}{cccc} \dot{y}_w & y_w & \dot{\psi}_w & \psi_w \end{array}]^T \tag{3.3.3}$$

$$\dot{x} = [\begin{array}{cccc} \dot{x}_1 & \dot{x}_2 & \dot{x}_3 & \dot{x}_4 \end{array}]^T = [\begin{array}{cccc} \ddot{y}_w & \dot{y}_w & \ddot{\psi}_w & \dot{\psi}_w \end{array}]^T \tag{3.3.4}$$

$$u = [\begin{array}{cc} F_y & T_\psi \end{array}]^T \tag{3.3.5}$$

and the system matrix (*Aw*), input matrix (*Bw*), output matrix (*Cw*) and feedforward matrix (*Dw*) as below:

$$A_w = \begin{bmatrix} \dfrac{-2f_{22}}{mV} & 0 & 0 & \dfrac{2f_{22}}{m} \\ 1 & 0 & 0 & 0 \\ 0 & \dfrac{-2f_{11}l\lambda}{I_\psi r} & \dfrac{-2f_{11}l^2}{I_\psi V} & 0 \\ 0 & 0 & 1 & 0 \end{bmatrix} \tag{3.3.6}$$

$$B_w = \begin{bmatrix} \dfrac{1}{m} & 0 \\ 0 & 0 \\ 0 & \dfrac{1}{I_\psi} \\ 0 & 0 \end{bmatrix} \tag{3.3.7}$$

$$C_w = \begin{bmatrix} 0 & 1 & 0 & 0 \\ 0 & 0 & 0 & 1 \end{bmatrix} \tag{3.3.8}$$

$$D_w = \begin{bmatrix} 0 & 0 \\ 0 & 0 \end{bmatrix} \tag{3.3.9}$$

3.3 THREE-AXLE RAILWAY VEHICLE

3.3.1 MATHEMATICAL DESCRIPTION

For the two axle railway vehicle system mathematical equations can be extended from equations (3.1) and (3.2) that represent the dynamic characteristics of a single solid axle wheelset. By adding another solid axle wheelset and a vehicle body into the previous single solid axle wheelset, the mathematical description of the three axle vehicle can be determined as below:

i. Front wheelset:

$$m\ddot{y}_{w1} = \left[\frac{-2f_{22}}{V} - C_w\right]\dot{y}_{w1} - K_w y_{w1} + 2f_{22}\psi_{w1} + C_w\dot{y}_v + K_w y_v + C_w l_b\dot{\psi}_v + K_w l_b\psi_v \tag{3.4.1}$$

$$I_w\ddot{\psi}_{w1} = \frac{-2f_{11}l\lambda}{r}y_{w1} - \frac{2f_{11}l^2}{V}\dot{\psi}_{w1} + T_{\psi 1} \tag{3.4.2}$$

ii. Middle wheelset:

$$m\ddot{y}_{w2} = \left[\frac{-2f_{22}}{V} - C_w\right]\dot{y}_{w2} - K_w y_{w2} + 2f_{22}\psi_{w2} + C_w\dot{y}_v + K_w y_v - C_w l_b\dot{\psi}_v - K_w l_b\psi_v \tag{3.4.3}$$

$$I_w\ddot{\psi}_{w2} = \frac{-2f_{11}l\lambda}{r}y_{w2} - \frac{2f_{11}l^2}{V}\dot{\psi}_{w2} + T_{\psi 2} \tag{3.4.4}$$

iii. Rear wheelset

$$m\ddot{y}_{w3} = \left[\frac{-2f_{22}}{V} - C_w\right]\dot{y}_{w3} - K_w y_{w3} + 2f_{22}\psi_{w3} + C_w\dot{y}_v + K_w y_v - C_w l_b\dot{\psi}_v - K_w l_b\psi_v \tag{3.4.5}$$

$$I_w\ddot{\psi}_{w3} = \frac{-2f_{11}l\lambda}{r}y_{w3} - \frac{2f_{11}l^2}{V}\dot{\psi}_{w3} + T_{\psi 3} \tag{3.4.6}$$

iv. Vehicle body:

$$m\ddot{y}_v = C_w\dot{y}_{w1} + K_w y_{w1} + C_w\dot{y}_{w2} + K_w y_{w2} + C_w\dot{y}_{w3} + K_w y_{w3} - 2C_w\dot{y}_v - 2K_w y_v \qquad (3.4.7)$$

$$I_v\ddot{\psi}_v = C_w l_b\dot{y}_{w1} + K_w l_b y_{w1} - C_w l_b\dot{y}_{w2} - K_w l_b y_{w2} - C_w l_b\dot{y}_{w3} - K_w l_b y_{w3}$$
$$-2C_w\, l_b^2\dot{\psi}_v - 2K_w\, l_b^2\dot{\psi}_v - T_{\psi 1} - T_{\psi 2} \qquad (3.4.8)$$

3.3.2 STATE-SPACE REPRESENTATION

The dynamic equations of two axle railway vehicle are similar to the ones for solid axle wheelset. But, instead of only having system matrix, input matrix and output matrix, the state equation of two axle vehicle has another matrix component to describe the deterministic track input into the system; curve radius and cant angle. The standard state equation in equation (3.3.1) is modified as below [16]:

$$\dot{x} = A_a x + B_a u + G_a w \qquad (3.5.1)$$

where;

$$x = [\ \dot{y}_{w1}\ \ y_{w1}\ \ \dot{\psi}_{w1}\ \ \psi_{w1}\ \ \dot{y}_{w2}\ \ y_{w2}\ \ \dot{\psi}_{w2}\ \ \psi_{w2}\ \ \dot{y}_{w3}\ \ y_{w3}\ \ \dot{\psi}_{w3}\ \ \psi_{w3}\ \ \dot{y}_v\ \ y_v\ \ \dot{\psi}_v\ \ \psi_v\ ]^T \qquad (3.5.2)$$

$$\dot{x} = [\ \ddot{y}_{w1}\ \ \dot{y}_{w1}\ \ \ddot{\psi}_{w1}\ \ \dot{\psi}_{w1}\ \ \ddot{y}_{w2}\ \ \dot{y}_{w2}\ \ \ddot{\psi}_{w2}\ \ \dot{\psi}_{w2}\ \ \ddot{y}_{w3}\ \ \dot{y}_{w3}\ \ \ddot{\psi}_{w3}\ \ \dot{\psi}_{w3}\ \ \ddot{y}_v\ \ \dot{y}_v\ \ \ddot{\psi}_v\ \ \dot{\psi}_v\ ]^T \qquad (3.5.3)$$

$$u = [\ T_{\psi 1}\ \ T_{\psi 2}\ \ T_{\psi 3}\ ]^T \qquad (3.5.4)$$

$$w = [\ 1/R_1\ \ \theta_{c1}\ \ 1/R_2\ \ \theta_{c2}\ \ 1/R_3\ \ \theta_{c3}\ ]^T \qquad (3.5.5)$$

and system matrix *Aa* is given below:

$$A=\begin{bmatrix}
a_{1,1} & a_{1,2} & 0 & a_{1,4} & 0 & 0 & 0 & 0 & 0 & 0 & 0 & 0 & a_{1,13} & a_{1,14} & a_{1,15} & a_{1,16}\\
1 & 0 & 0 & 0 & 0 & 0 & 0 & 0 & 0 & 0 & 0 & 0 & 0 & 0 & 0 & 0\\
0 & a_{3,2} & a_{3,3} & 0 & 0 & 0 & 0 & 0 & 0 & 0 & 0 & 0 & 0 & 0 & 0 & 0\\
0 & 0 & 1 & 0 & 0 & 0 & 0 & 0 & 0 & 0 & 0 & 0 & 0 & 0 & 0 & 0\\
0 & 0 & 0 & 0 & a_{5,5} & a_{5,6} & 0 & a_{5,8} & 0 & 0 & 0 & 0 & a_{5,13} & a_{5,14} & a_{5,15} & a_{5,16}\\
0 & 0 & 0 & 0 & 1 & 0 & 0 & 0 & 0 & 0 & 0 & 0 & 0 & 0 & 0 & 0\\
0 & 0 & 0 & 0 & 0 & a_{7,6} & a_{7,7} & 0 & 0 & 0 & 0 & 0 & 0 & 0 & 0 & 0\\
0 & 0 & 0 & 0 & 0 & 0 & 1 & 0 & 0 & 0 & 0 & 0 & 0 & 0 & 0 & 0\\
0 & 0 & 0 & 0 & 0 & 0 & 0 & 0 & a_{9,9} & a_{9,10} & 0 & a_{9,12} & a_{9,13} & a_{9,14} & a_{9,15} & a_{9,16}\\
0 & 0 & 0 & 0 & 0 & 0 & 0 & 0 & 1 & 0 & 0 & 0 & 0 & 0 & 0 & 0\\
0 & 0 & 0 & 0 & 0 & 0 & 0 & 0 & 0 & a_{11,10} & a_{11,11} & 0 & 0 & 0 & 0 & 0\\
0 & 0 & 0 & 0 & 0 & 0 & 0 & 0 & 0 & 0 & 1 & 0 & 0 & 0 & 0 & 0\\
a_{13,1} & a_{13,2} & 0 & 0 & a_{13,5} & a_{13,6} & 0 & 0 & a_{13,9} & a_{13,10} & 0 & 0 & a_{13,13} & a_{13,14} & 0 & 0\\
0 & 0 & 0 & 0 & 0 & 0 & 0 & 0 & 0 & 0 & 0 & 0 & 1 & 0 & 0 & 0\\
a_{15,1} & a_{15,2} & 0 & 0 & a_{15,5} & a_{15,6} & 0 & 0 & a_{15,9} & a_{15,10} & 0 & 0 & 0 & 0 & a_{15,15} & a_{15,16}\\
0 & 0 & 0 & 0 & 0 & 0 & 0 & 0 & 0 & 0 & 0 & 0 & 0 & 0 & 1 & 0
\end{bmatrix} \tag{3.5.6}$$

where;

$a_{1,1}$, $a_{5,5}$, $a_{9,9}$ $= \dfrac{-2f_{22}}{mV} - \dfrac{C_w}{m}$

$a_{1,2}$, $a_{5,6}$, $a_{9,10}$ $= \dfrac{-K_w}{m}$

$a_{1,4}$, $a_{5,8}$, $a_{9,12}$ $= = \dfrac{2f_{22}}{m}$

$a_{1,13}$, $a_{5,13}$, $a_{9,13} = \dfrac{C_w}{m}$

$a_{1,14}$, $a_{5,14}$, $a_{9,14} = \dfrac{K_w}{m}$

$a_{1,15}$, $-a_{5,15}$, $-a_{9,15} = \dfrac{K_w l_b}{m}$

$a_{3,2}$, $a_{7,6}$, $a_{11,10} = \dfrac{-2f_{11}l\lambda}{I_w r}$

$a_{3,3}$, $a_{7,7}$, $a_{9,9} = \dfrac{-2f_{11}l^2}{I_w V}$

$a_{13,1}$, $a_{13,5}$, $a_{13,9}$ = $\frac{C_w}{m_v}$

$a_{13,2}$, $a_{13,6}$, $a_{13,9}$ = $\frac{K_w}{m_v}$

$a_{13,13}$ = $\frac{-2C_w}{m_v}$

$a_{13,14}$ = $\frac{-2K_w}{m_v}$

$a_{15,1}$, $-a_{15,5}$, $-a_{15,9}$ = $\frac{C_w l_b}{I_V}$

$a_{15,2}$, $-a_{15,6}$, $-a_{15,10}$ = $\frac{K_w l_b}{I_v}$

$a_{15,15}$ = $\frac{-2C_w lb^2}{I_v}$

$a_{15,16}$ = $\frac{-2K_w lb^2}{I_v}$

and input matrix, *Ba* is:

$$B_a = \begin{bmatrix} 0 & 0 & 0 \\ 0 & 0 & 0 \\ 1/I_w & 0 & 0 \\ 0 & 0 & 0 \\ 0 & 0 & 0 \\ 0 & 0 & 0 \\ 0 & 1/I_w & 0 \\ 0 & 0 & 0 \\ 0 & 0 & 0 \\ 0 & 0 & 0 \\ 0 & 0 & 1/I_w \\ 0 & 0 & 0 \\ 0 & 0 & 0 \\ 0 & 0 & 0 \\ -1/I_v & -1/I_v & -1/I_v \\ 0 & 0 & 0 \end{bmatrix} \tag{3.5.7}$$

and finally disturbance matrix, *Ga* is:

$$G_a = \begin{bmatrix} V^2 & -g & 0 & 0 & 0 & 0 & 0 & 0 & 0 \\ 0 & 0 & -1 & 0 & 0 & 0 & 0 & 0 & 0 \\ \frac{2f_{11}l^2}{I_w} & 0 & 0 & 0 & 0 & 0 & 0 & 0 & 0 \\ 0 & 0 & 0 & 0 & 0 & 0 & 0 & 0 & 0 \\ 0 & 0 & 0 & V^2 & -g & 0 & 0 & 0 & 0 \\ 0 & 0 & 0 & 0 & 0 & -1 & 0 & 0 & 0 \\ 0 & 0 & 0 & \frac{2f_{11}l^2}{I_w} & 0 & 0 & 0 & 0 & 0 \\ 0 & 0 & 0 & 0 & 0 & 0 & 0 & 0 & 0 \\ 0 & 0 & 0 & 0 & 0 & 0 & V^2 & -g & 0 \\ 0 & 0 & 0 & 0 & 0 & 0 & 0 & 0 & -1 \\ 0 & 0 & 0 & 0 & 0 & 0 & \frac{2f_{11}l^2}{I_w} & 0 & 0 \\ 0 & 0 & 0 & 0 & 0 & 0 & 0 & 0 & 0 \\ \frac{V^2}{3} & \frac{-g}{3} & 0 & \frac{V^2}{3} & \frac{-g}{3} & 0 & \frac{V^2}{3} & \frac{-g}{3} & 0 \\ 0 & 0 & \frac{-1}{2} & 0 & 0 & \frac{-1}{2} & 0 & 0 & \frac{-1}{2} \\ 0 & 0 & 0 & 0 & 0 & 0 & 0 & 0 & 0 \\ 0 & 0 & 0 & 0 & 0 & 0 & 0 & 0 & 0 \end{bmatrix} \tag{3.5.8}$$

3.3.3 VEHICLE PARAMETER VALUES FOR SIMULATION

The parameters values for two axle vehicle simulation are referred to [16] as shown in Table 3.1 below:

Table 3.1: Two-axle Railway Vehicle Parameters Symbol

Symbol	Description	Value
y_{w1}, y_{w2} , y_v	Lateral displacement of front, middle, rear wheelset and body	-
ψ_{w1}, ψ_{w2}, ψ_v	Yaw displacement of front, middle, rear and body	-
V	Vehicle velocity	60 m/s, 80m/s, 100m/s
m , m_v	Wheelset and vehicle mass	1250 kg 13500 kg
I_w I_v	Wheelset and vehicle inertia	700 kgm^2 $17x10^4$ kgm^2
l_b	Half spacing between two wheelset	3.7 m
K_w	Lateral stiffness per wheelset	230 kN/m
C_w	Lateral stiffness per wheelset	50 kN s/m
r	Wheel radius	0.45 m
λ	Conicity	0.2
l	Half gauge of wheelset	0.7 m
f_{11}	Longitudinal creep coefficient	10 MN
f_{22}	Lateral creep coefficient	10 MN
R_1, R_2	Radius of the curved track at the front and rear wheelsets	1000 m, 1500 m, 2000 m
θ_1, θ_2	Cant angle of the curved track at the front and rear wheelsets	7^o, 14^o, 21^o
$T_{\psi 1}$, $T_{\psi 2}$	Controlled torque input for front and rear wheelsets	-

g	Gravity	$9.8\ m/s^2$

CHAPTER 4

CONTROLLER DESIGN

4.1 INTRODUCTION

In this chapter, the controller design will be discussed. The type of controller used for the system also will be discussed. The 16 states for three axle railway vehicle also will be shown as the system consists of three wheelsets. Lastly in this chapter, LQR controller will be briefly explained.

4.2 MODERN CONTROL

Nowadays, many type of control modern have been established, to replace the conventional control method such as PID and other. Controller such as LQR, pole placement controller, optimal controller and robust controller are commonly used due to the simpler and easier solution and method. But for each controller, there is advantage and disadvantage. So, the controller selection is the most important thing to do to make sure the controller can fulfill the requirement for the system. In this project, the best controller to be used is optimal controller. Here is some briefly explanation about the optimal controller:

Optimal controller

Optimal control theory is a mathematical optimization method for deriving control policies. Optimal control deals with the problem of finding a control law for a given system such that a certain optimality criterion is achieved. A control problem includes a cost functional that is a function of state and control variables. An optimal control is a set of differential equations describing the paths of the control variables that minimize the cost functional.

Optimal controller was chosen in this project due to several issues that must be addressed. The controller is designed for the active steering of railway vehicle. The most important thing is, the controller must stabilize the system and the closed loop system should be robust against variation of operational parameters such as wheel conicity and creepage coefficients. Secondly, the controller to be designed should not interfere with the natural curving action of the wheelsets. So, optimal controller is the most suitable to be used in this project.

A general diagram of the control structure is shown in Figure 5.1 [17]. The input of the system is the track input (deterministic input) which the curve radius and the cant angle are predetermined according to the standard provided by responsible bodies. The system information consists of system matrix, input matrix, output matrix and disturbance matrix (in state space representation. Sensors are applied to sense appropriate parameters to be measured and feedback into the system. Actuators are used to give any physical changes towards the controlled system. The actuator type can be either hydraulic, pneumatic, motor driven or combination between them [1].

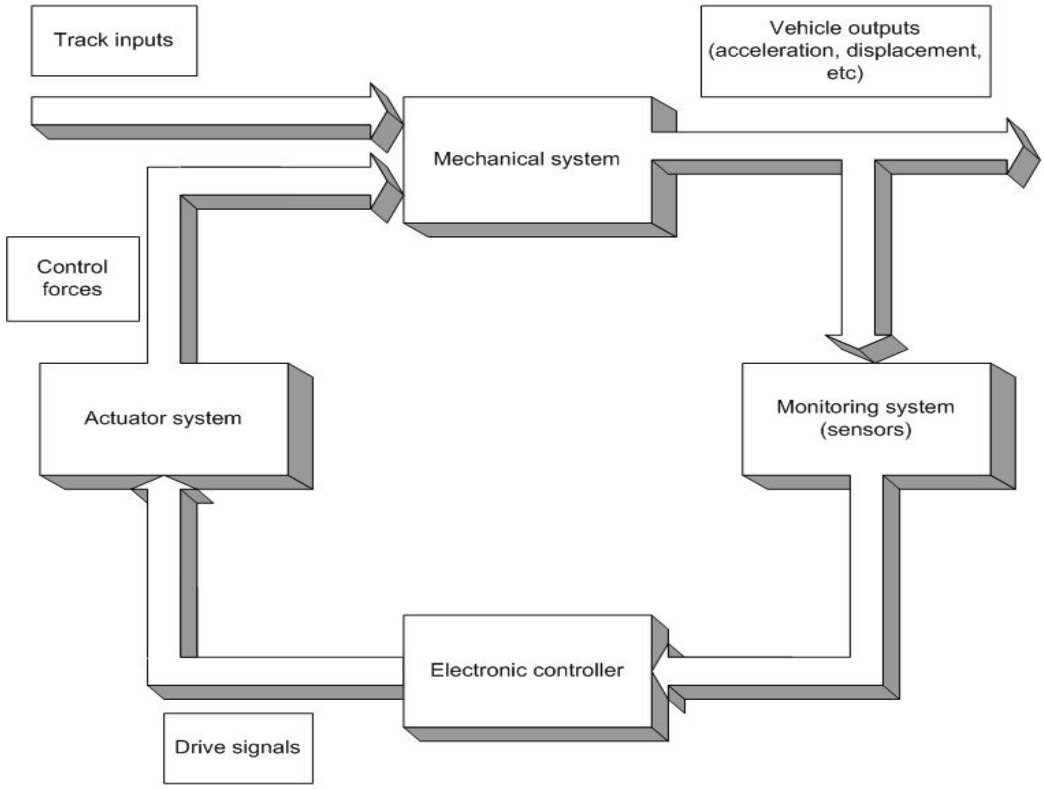

Figure 4.1: Control Structure Diagram

4.3 Linear Quadratic Regulator

Optimal control is concerned with operating a dynamic system at minimum cost. Linear quadratic regulator (LQR) is the case where the system dynamics are described by a set of linear differential equations and the cost, *J* is described by a quadratic functional.

The settings of the LQR controller are found by using a mathematical algorithm that minimizes the cost function with weighting factors determined by the controller designer (human). The cost function is often defined as a sum of the deviations of key measurements from their desired values. In effect, this algorithm will then find those controller settings that minimize the undesired deviations.

The LQR algorithm takes care of the tedious work to optimizing the controller. However, the controller designer still needs to specify the weighting

Vehicle system factors and compare the results with the specified design goals. As a result, controller synthesis will still be an iterative process where the designer judges the designed optimal controllers through simulation and then adjusts the weighting factors to get a controller more in line with the specified design goals.

When designing an optimal controller, the system is assumed to be linear and has a state equation in the form below:

$$\dot{x} = Ax + Bu \tag{4.1}$$

$$y = Cx \tag{4.2}$$

The control law is chosen such that it minimizes the cost function,

$$J = \int \left(y^T(t) \cdot Q \cdot y(t) + u^T(t) \cdot R \cdot u(t) \right) dt \tag{4.3}$$

where y represents the selected states to be controlled. In this simulation study, y is described as below:

$$y = \begin{bmatrix} y_{w1} & \theta_{w1} & y_{w2} & \theta_{w2} & y_{w3} & \theta_{w3} \end{bmatrix}^T \tag{4.4}$$

The weighting matrices, Q and R are crucial to get a good optimal controller. In this study, R is fixed at 10^{-12} to maintain a good tracking performance and Q is to be adjusted. After several attempts, the appropriate values of Q for three-axle is determined.

$$Q = diag\begin{bmatrix} 100 & 10 & 100 & 10 & 100 & 10 \end{bmatrix} \tag{4.5}$$

$$R = diag\begin{bmatrix} 10^{-12} & 10^{-12} & 10^{-12} \end{bmatrix} \tag{4.6}$$

The control law is given Equation 5.6 below [18]:

$$u(t) = -K(t)\, x(t) \tag{4.7}$$

The feedback gain matrix K is described below:

$$K(t) = -R^{-1}B^{T}(t)\,P_r(t) \tag{4.8}$$

and Pr is obtained by solving Ricatti equation below:

$$\dot{P}_r(t) = -P_r(t)A(t) - A^{T}(t)P_r(t) - Q + P_r(t)\,B(t)\,R^{-1}B^{T}(t)\,P_r(t) \tag{4.9}$$

CHAPTER 5

RESULT AND DISCUSSIONS

5.1 INTRODUCTION

This chapter consists of the discussion about the simulations of the active suspension for three axle railway vehicle. From the simulation result, the parameter's value will be varied and will be compared to analyze the best parameter's criteria that will effects the better train performance. The parameters that will be tested are cant angle, curve radius, and train velocity. Simulation result will be divided to four, which are control torque, lateral displacement, yaw angle, and body vehicle acceleration.

5.2 TRACK INPUT PARAMETER

The suspension arrangement for two-axle vehicle with active suspension is shown in Figure 2.8. Figure 6.1 (a), 6.1 (b), 6.1 (c), 6.1 (d), 6.1 (e), 6.1 (f), and Figure 6.1(g) show the input for different value of parameters. The standard railway track profile used in these simulations is shown in Figure 6.4(a) which is the curved track with radius value is 1500 meters, vehicle velocity is 60 m/s and cant angle is 7 degree. All of the inputs will be connected to straight tracks on either end via one second transition is selected to study the control performance on curves. The input will give effect to control torque, lateral displacement, yaw angle and vehicle acceleration result that will be shown in the next subchapter.

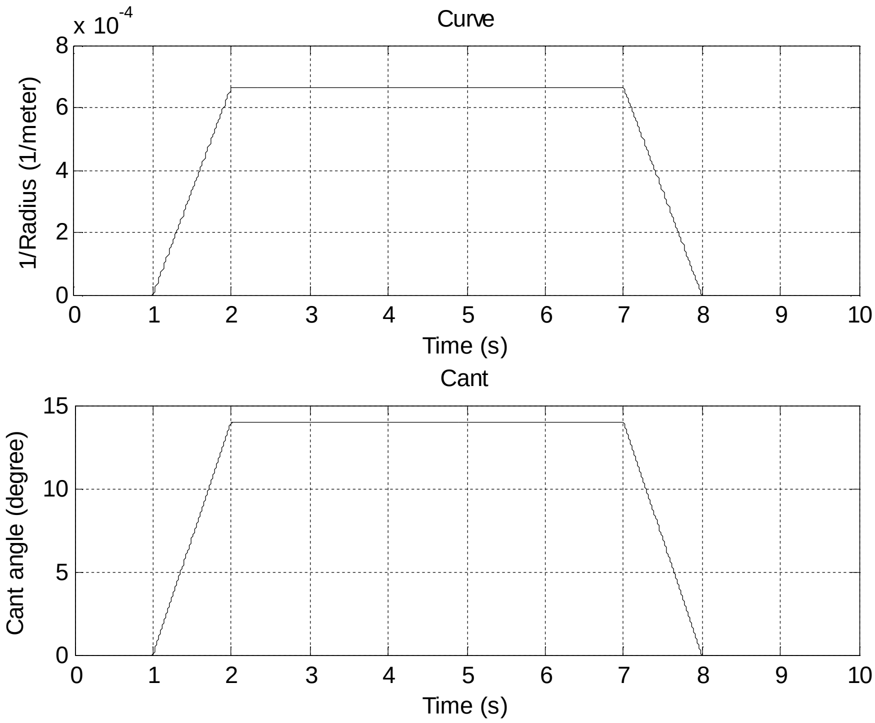

Figure 5.1(a): Input for standard parameter value

Figure 5.1(b) and 5.1(c) show the graph input for different cant angle value, from 14 degree to 7 and 21 degree, without changing the standard velocity and radius parameters value.

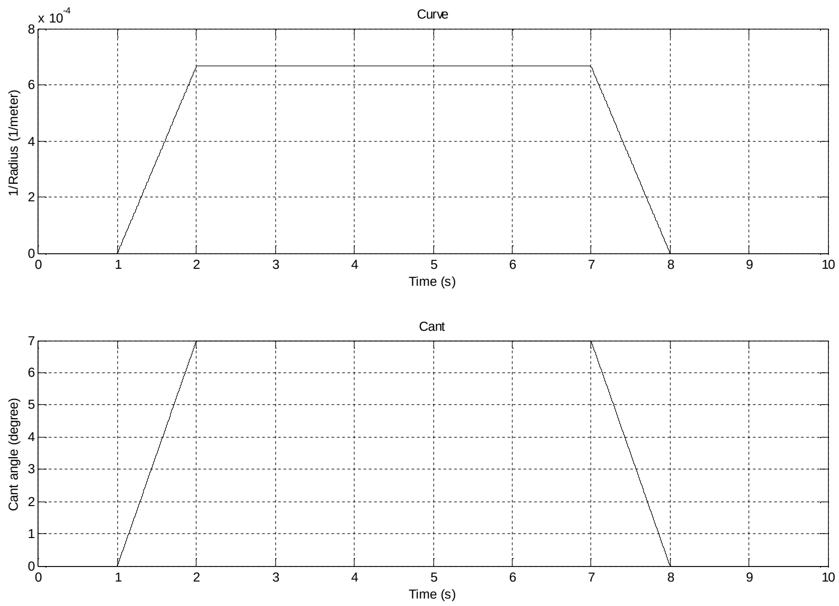

Figure 5.1(b): Input for cant angle at 7 degree

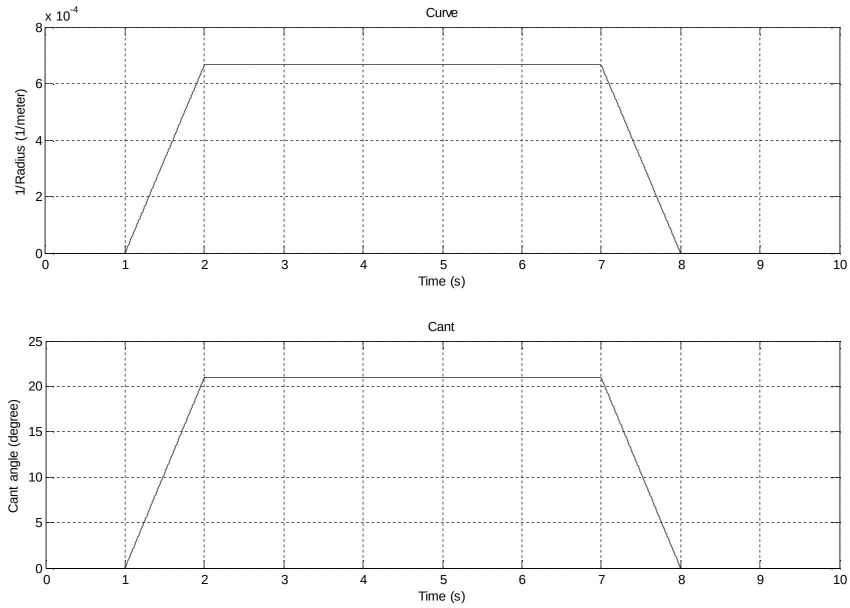

Figure 5.1(c): Input for cant angle at 21 degree

Figure 5.1(d) and 5.1(e) show the graph input for different curve radius value, from 1500 m to 1000 m and 2000 m, without changing the standard velocity and cant parameters value.

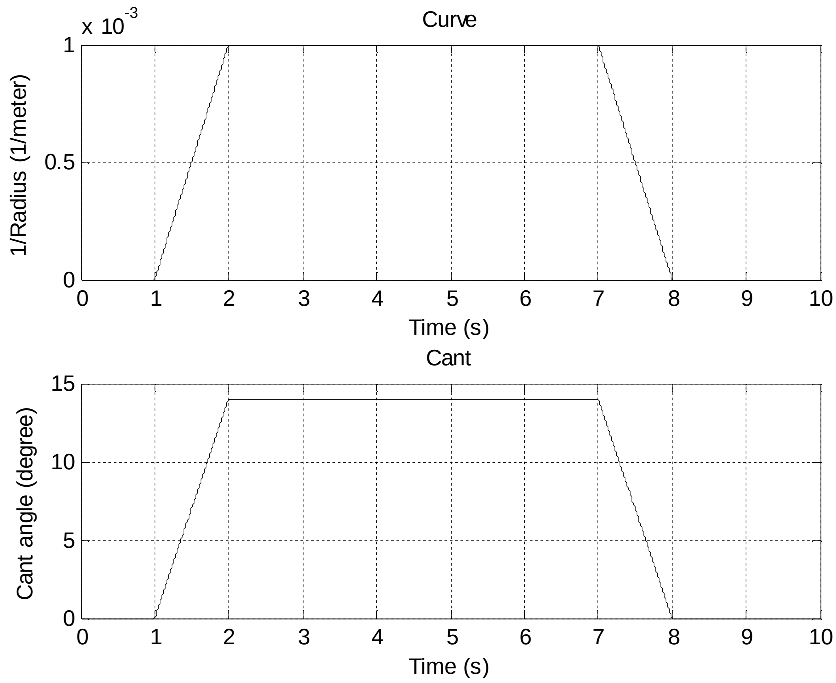

Figure 5.1(d): Input for curving track radius at 1000 m

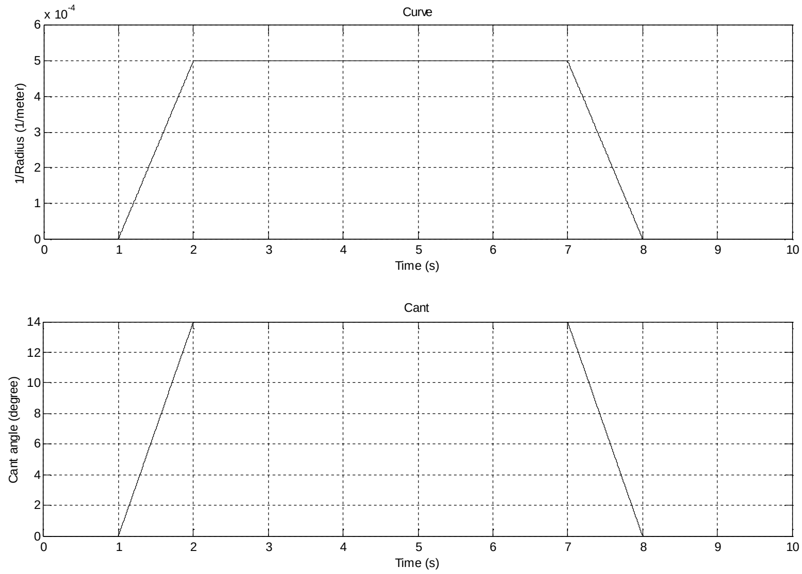

Figure 5.1(e): Input for curving track radius at 2000 m

Figure 5.1(f) and 5.1(g) show the graph input for different vehicle velocity value, from 60 m/s to 80 m/s and 100 m/s, without changing the standard radius and cant parameters value.

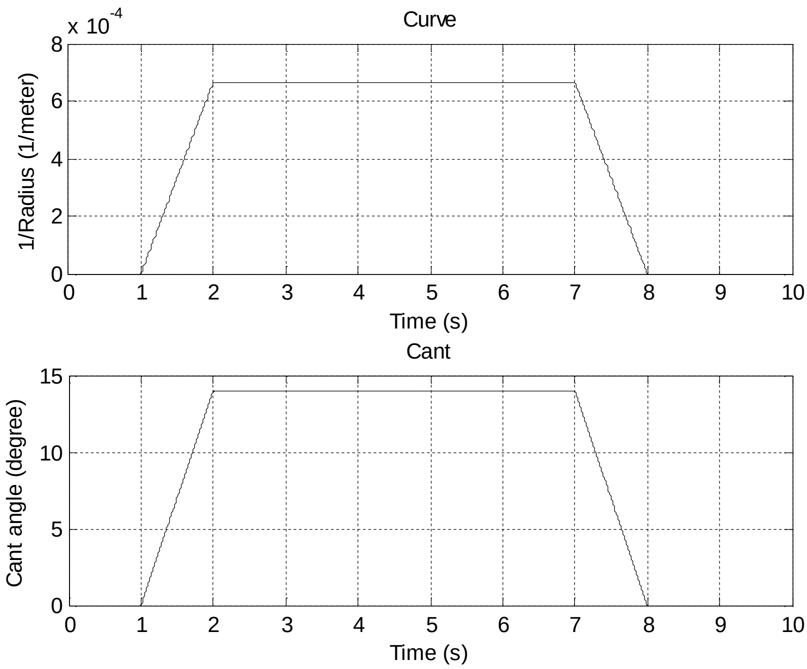

Figure 5.1(f): Input for vehicle velocity at 80 m/s

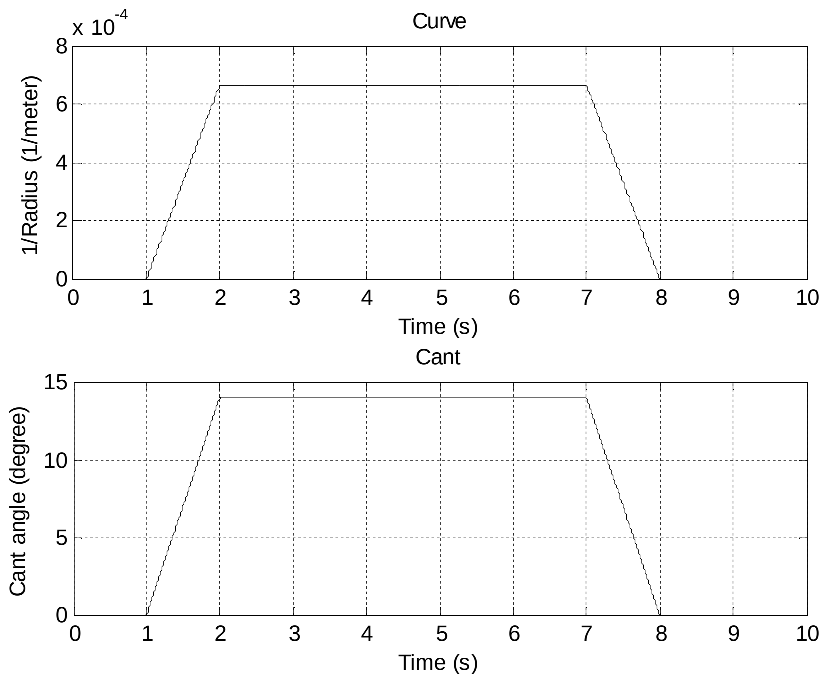

Figure 5.1(g): Input for vehicle velocity at 100 m/s

5.3 SIMULATION RESULT

5.3.1 CONTROL TORQUE

Control torque needs to be smaller to provide the stable active suspension. Figure 5.2(a) shows the control torque for the standard experiment by using cant angle at 14 degree, velocity at 60 m/s, and curve radius at 1500 m. The graph shows that the control torque required on the track is approximately 300 Nm for the third wheelset. First and second wheelset require smaller control torque which is approximately 175 Nm. During the transition from straight to curved track, the control torque acts at opposite direction from the curve transition.

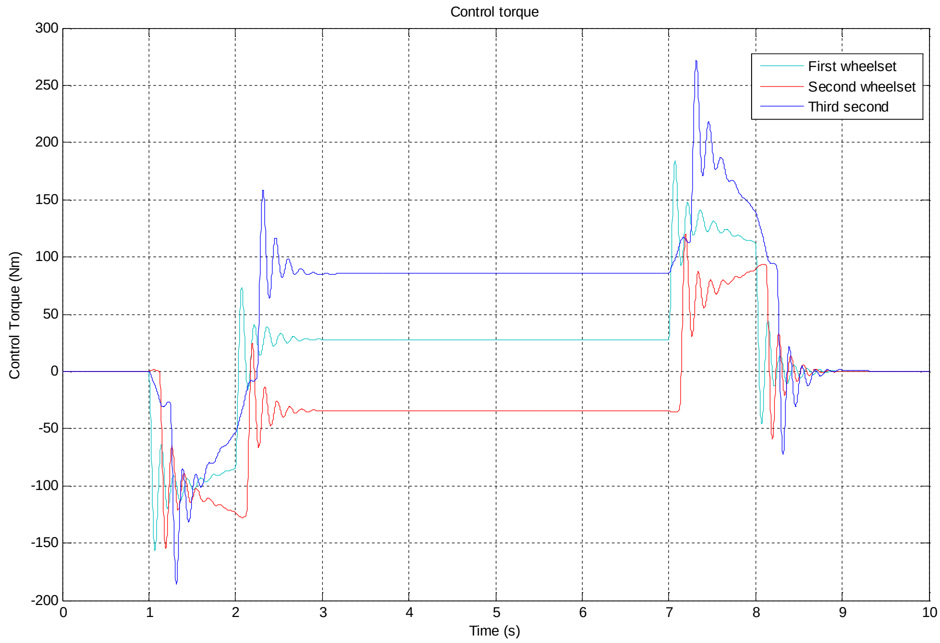

Figure 5.2(a): Control torque for standard parameters value

Figure 5.2(b) show control torque for parameter value for cant angle at 7 degree. The transition state for third wheelset goes until 680 Nm, second wheelset goes until approximately 400 Nm, and the first wheelset will give result approximately 500 Nm.

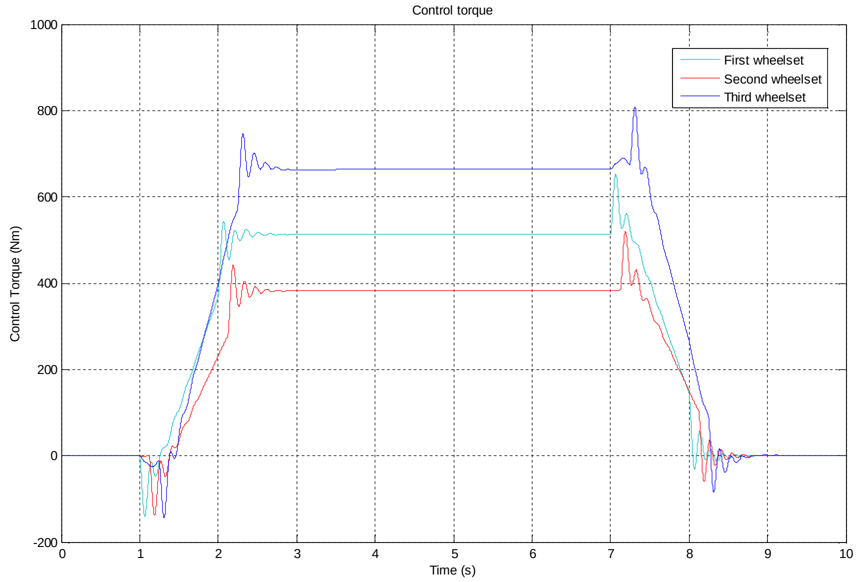

Figure 5.2(b): Control torque for cant angle at 7 degree

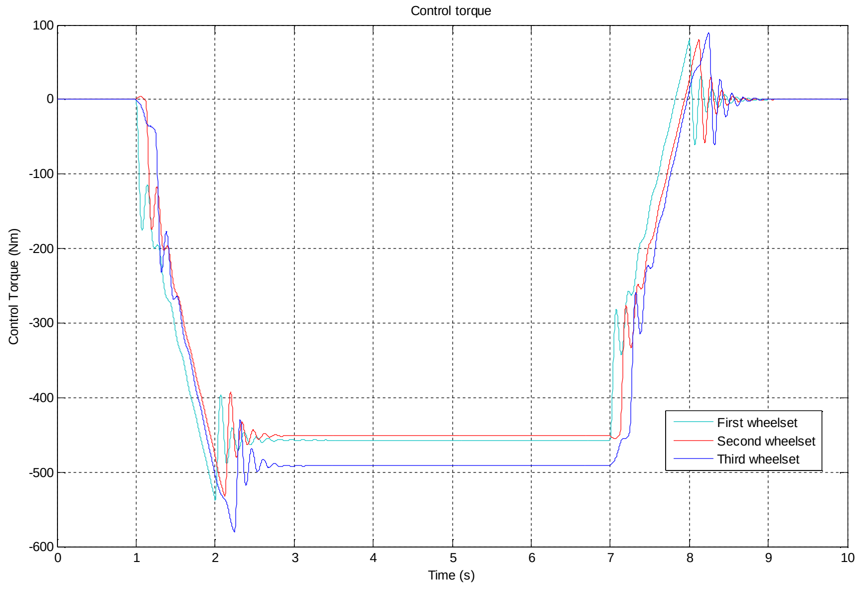

Figure 5.2(c): Control torque for cant angle at 21 degree

Figure 5.2(c) show control torque for parameter value for cant angle at 21 degree. The transition state for third wheelset goes until 580 Nm, and 530 Nm for both first and second wheelsets.

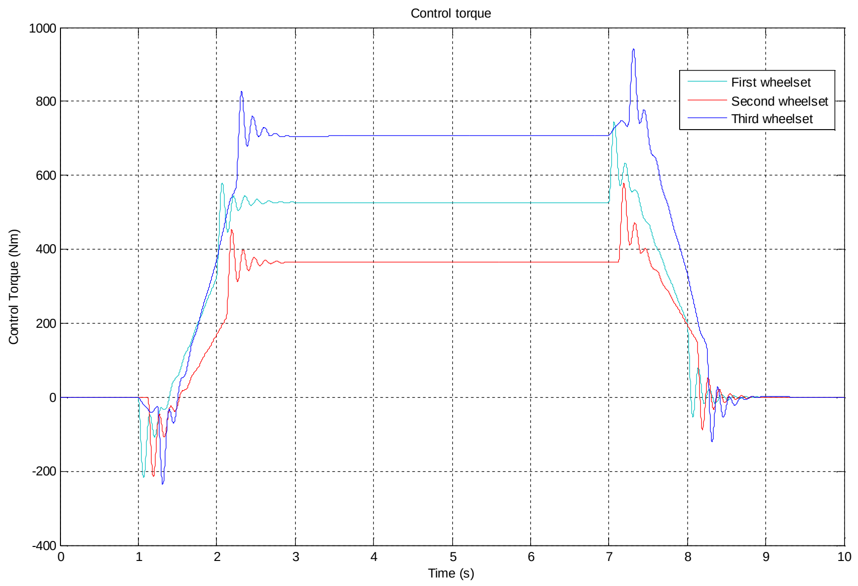

Figure 5.2(d): Control torque for curve radius at 1000 m

Figure 5.2(d) show the control torque for parameter value for curve radius at 1000 m. The result show that the transition state goes up to 800 Nm for the third wheelset. Second wheelset require smaller control torque which is approximately 400 Nm, and first wheelset goes until 600 Nm control torque. Figure 5.2(e) shows the result for the parameter value for curve radius at 2000 m. The result show that the transition state goes up to 350 Nm for all wheelsets.

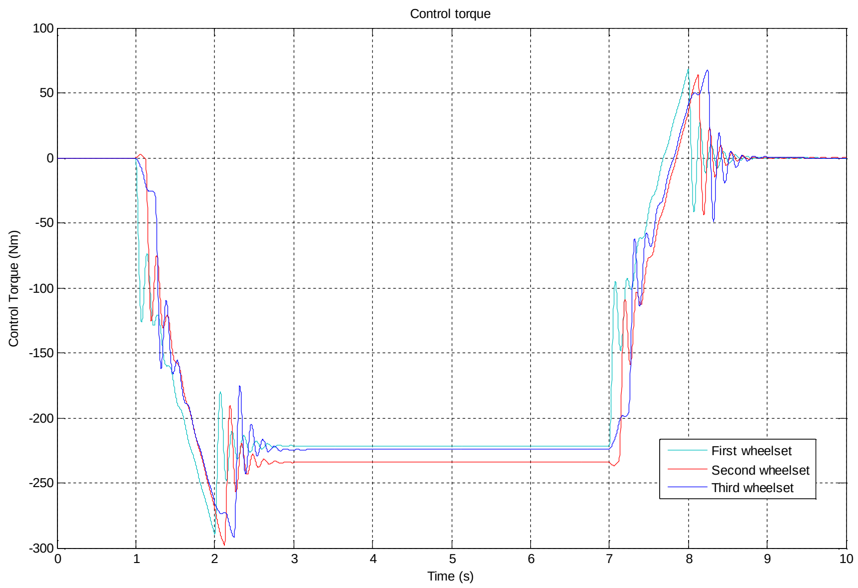

Figure 5.2(e): Control torque for curve radius at 2000 m

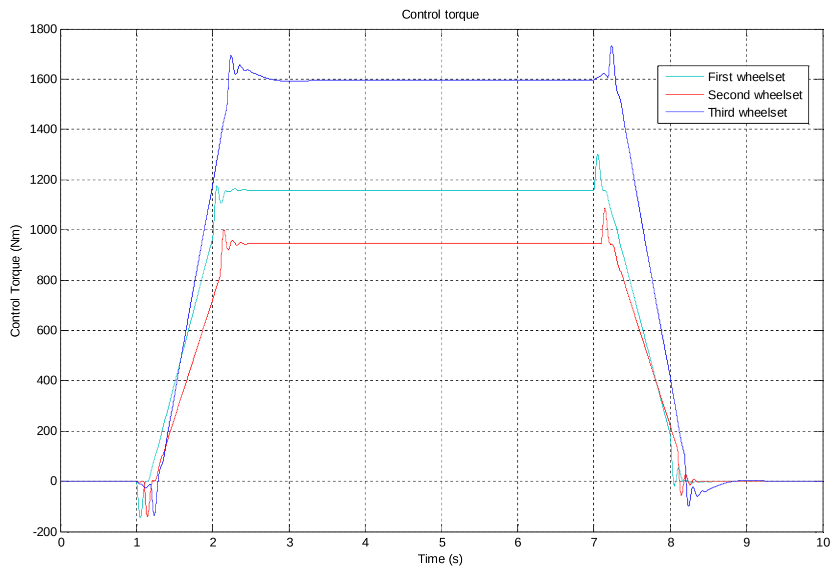

Figure 5.2(f): Control torque for vehicle velocity at 80 m/s

The Figure 5.2(f) shows the control torque for parameter value for velocity at 80 m/s. The result show that the transition state goes up to 1700 Nm for the third wheelset, 1200 Nm for the first wheelset, and 1000 Nm control torque for the second wheelset. The Figure 5.2(g) below show the control torque for parameter value for velocity at 100 m/s. The result show that the transition state goes up to 5000 Nm for the third wheelset, 3500 Nm for the first wheelset, and 3000 Nm control torque for the second wheelset.

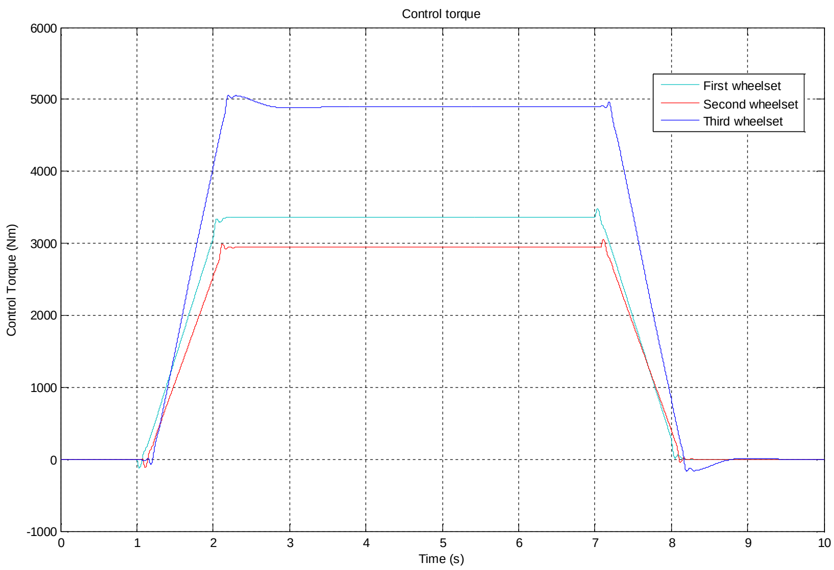

Figure 5.2(g): Control torque for vehicle velocity at 100 m/s

5.3.2 LATERAL DISPLACEMENT

Figure 5.3(a) show the lateral displacement for the standard value by using cant angle at 14 degree, velocity at 60 m/s, and curve radius at 1500 m. The graph show that the transition state goes up to 1.05 mm for all wheelsets. For the third wheelset, the steady state will go to zero while for first and second wheelsets, the steady state go up to 1.05 mm.

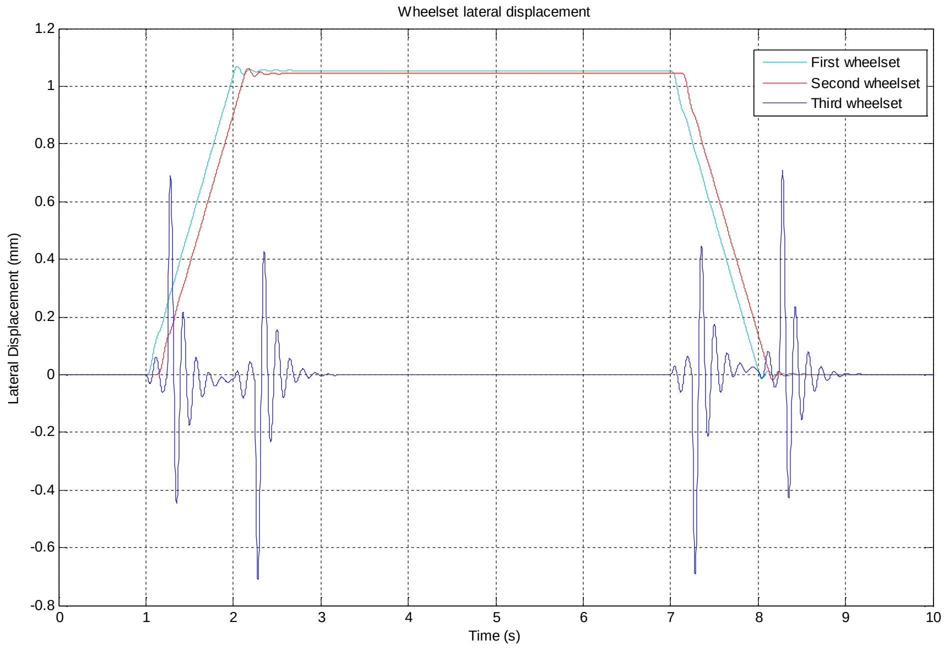

Figure 5.3(a): Lateral displacement for standard parameter value

Figure 5.3(b) shows the lateral displacement for parameter cant angle value at 7 degree. The transition states for first and second wheelsets go up until 1.1 mm. The third wheelset transition state goes until 1.4 mm. For the third wheelset, the steady state will go to zero while for first and second wheelsets, the steady state go up to 1.2 mm. Figure 5.3(c) shows the parameter cant angle value at 21 degree. The transition states for first and second wheelsets go up until 1 mm. The third wheelset transition state goes until 1.5 mm. For the third wheelset, the steady state will go to zero while for first and second wheelsets, the steady state go up to 1 mm.

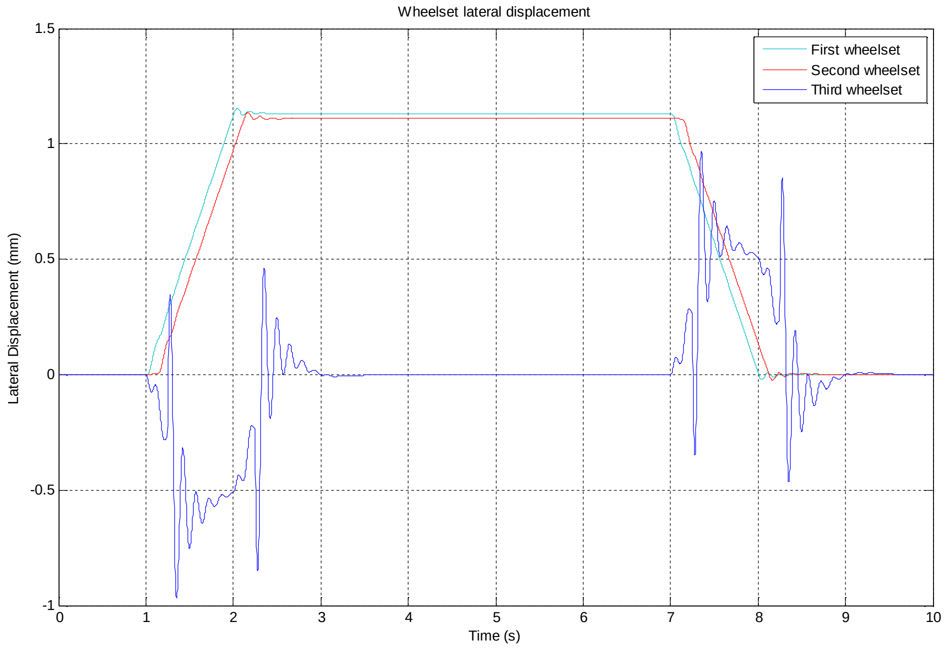

Figure 5.3(b): Lateral displacement for cant angle parameter value at 7 degree

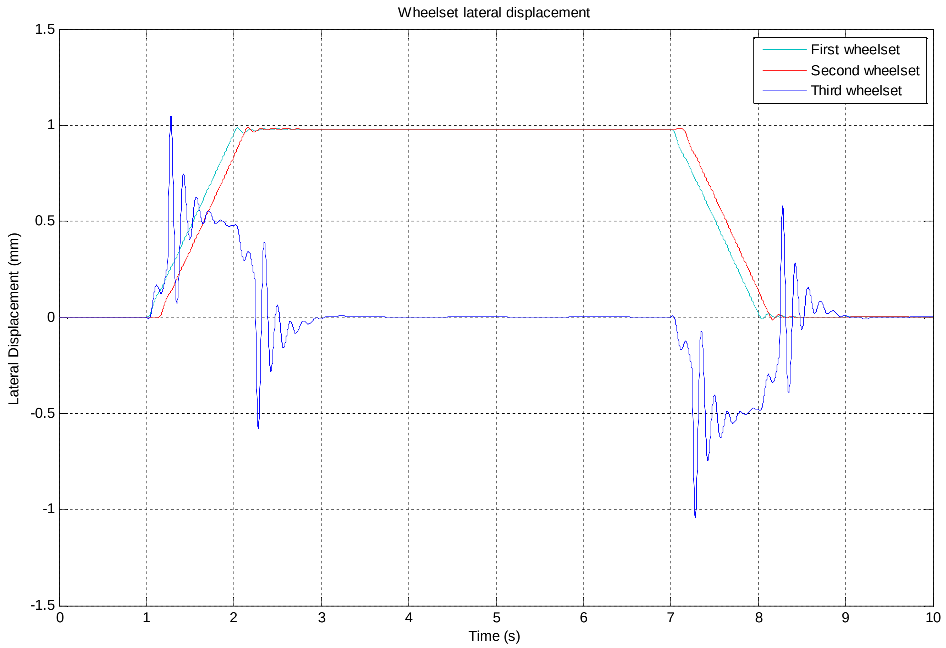

Figure 5.3(c): Lateral displacement for cant angle parameter value at 21 degree

Figure 5.3(d) show the lateral displacement for parameter curve track radius value at 1000 m. The transition states for first and second wheelsets go up until about 1.77 mm. The third wheelset transition state goes until 2.0 mm. For the third wheelset, the steady state will go to zero while for first and second wheelsets, the steady state go up to 1.77 mm. Figure 5.3(e) shows the parameter curve track radius at 2000 m. The transition states for first and second wheelsets go up until about 0.75 mm. The third wheelset transition state goes until 1.1 mm. For the third wheelset, the steady state will go to zero while for first and second wheelsets, the steady state go up to 0.75 mm.

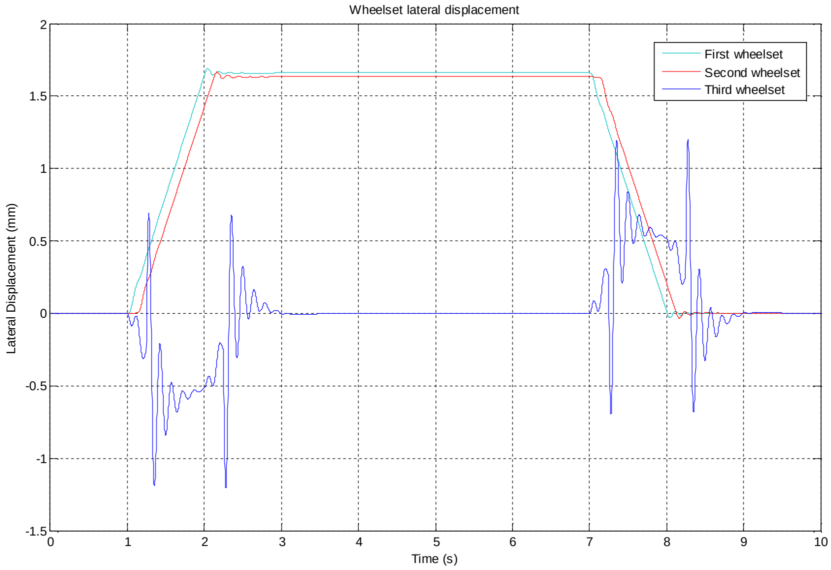

Figure 5.3(d): Lateral displacement for curve radius at 1000 m

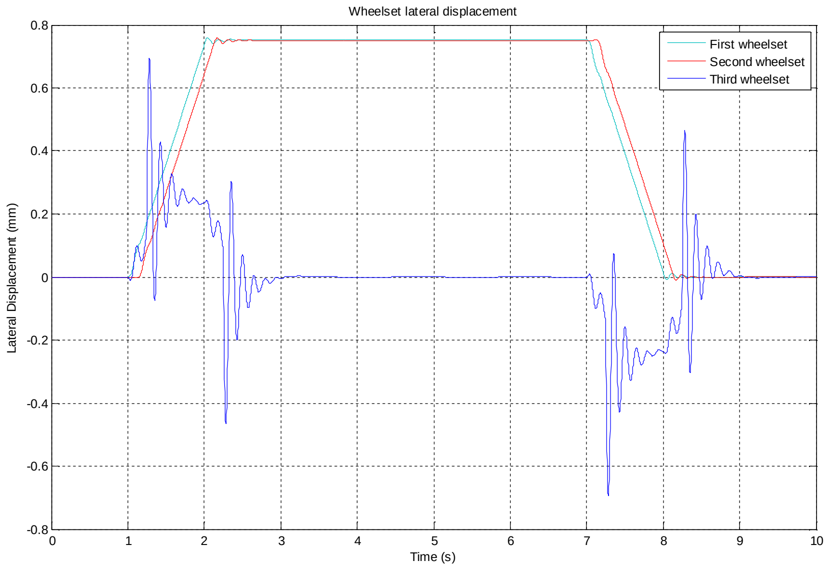

Figure 5.3(e): Lateral displacement for curve radius at 2000 m

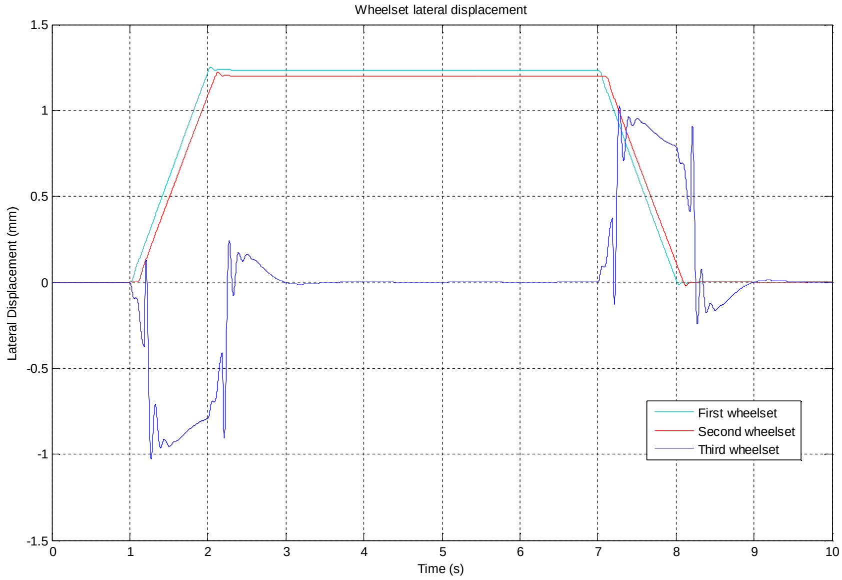

Figure 5.3(f): Lateral displacement for vehicle velocity at 800 m/s

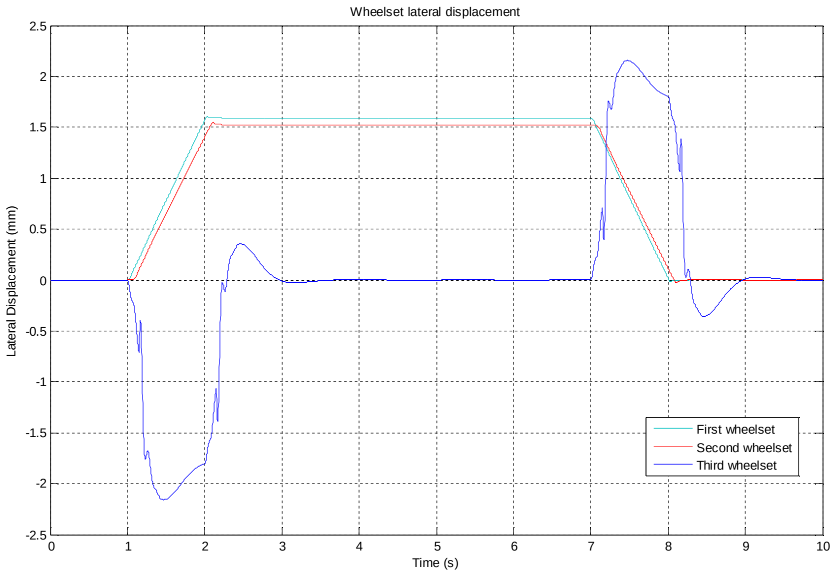

Figure 5.3(g): Lateral displacement for vehicle velocity at 100 m/s

Figure 5.3(f) show the lateral displacement for parameter vehicle velocity value at 80 m/s. The transition states for all wheelset are about same which are approximately 1.25 mm. For the third wheelset, the steady state will go to zero while for first and second wheelsets, the steady state go up to 1.25 mm. Figure 5.3(g) show the parameter vehicle velocity value at 100 m/s. Transition state for first wheelset is about 1.6 mm, second wheelset is about 1.5 mm and third wheelset is aobut 2.1 mm.

For the third wheelset, the steady state will go to zero while for first and second wheelsets, the steady state go up to approximately 1.6 mm.

5.2.3 YAW ANGLE

Figure 5.4(a) shows the graph of yaw angle result for standard parameter value. The transition states for all wheelset are about 0.006 mrad. The steady state for first wheelset is approximately to zero while steady state for second and third wheelset are approximately to 0.015 mrad.

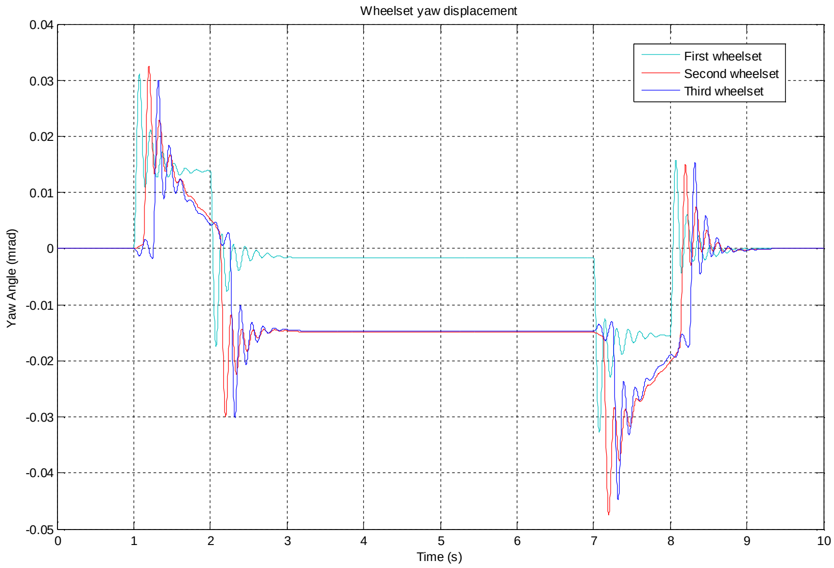

Figure 5.4(a): Yaw angle for standard parameter value

Figure 5.4(b) shows the graph of yaw angle result for parameter cant angle value at 7 degree. The transition states for second and third wheelsets are about 0.55 mrad. The transition state for first wheelset is approximately to 0.5 mrad. The steady state for first wheelset is approximately to 0.45 mrad while steady states for second and third wheelset are approximately to 0.5 mrad. Figure 5.4(c) shows the graph of yaw angle result for parameter cant angle value at 21 degree. The transition states for all wheelsets are about 0.55 mrad. The steady states for all wheelsets are approximately to 0.475 mrad.

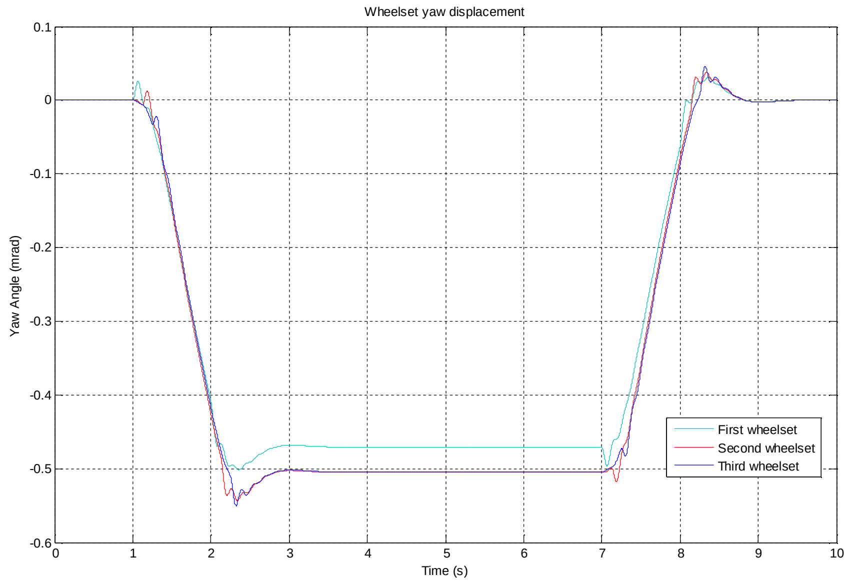

Figure 5.3(b): Yaw angle for parameter cant angle value at 7 degree

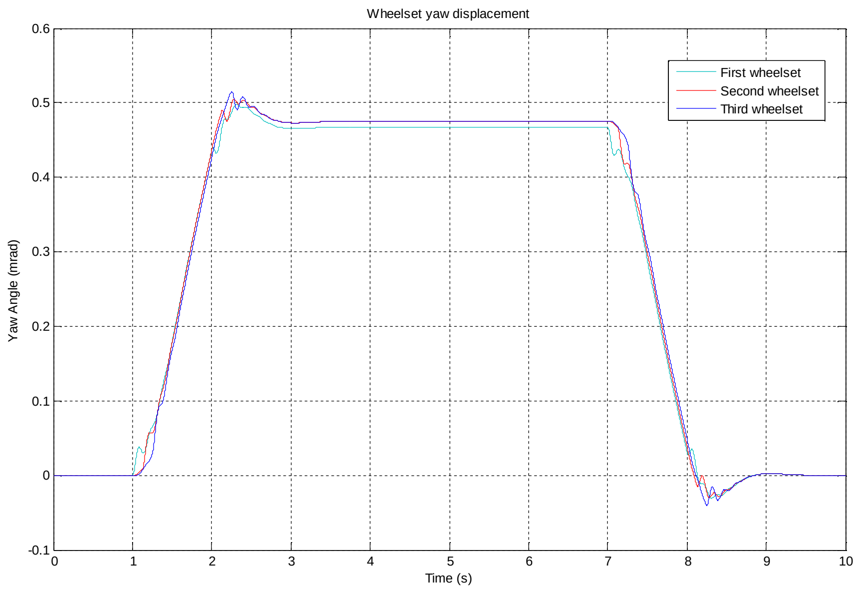

Figure 5.3(c): Yaw angle for parameter cant angle value at 21 degree

Figure 5.4(d) shows the graph of yaw angle result for parameter curving track radius value at 1000 m. The transition states for second and third wheelsets are about 0.56 mrad. The transition state for first wheelset is approximately to 0.5 mrad. The steady state for first wheelset is approximately to 0.45mrad while steady states for second and third wheelset are approximately to 0.51 mrad. Figure 5.4(e) shows the graph of yaw angle result for parameter curving track radius value at 2000 m. The transition states for all wheelsets are approximately 0.25 mrad. The steady states for all wheelsets are approximately to 0.22 mrad.

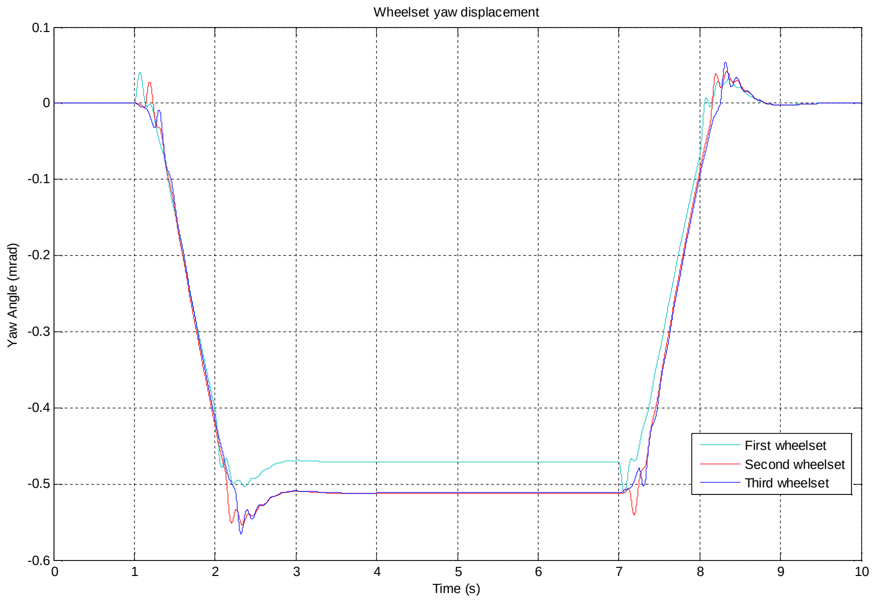

Figure 5.3(d): Yaw angle for parameter curving track radius at 1000 m

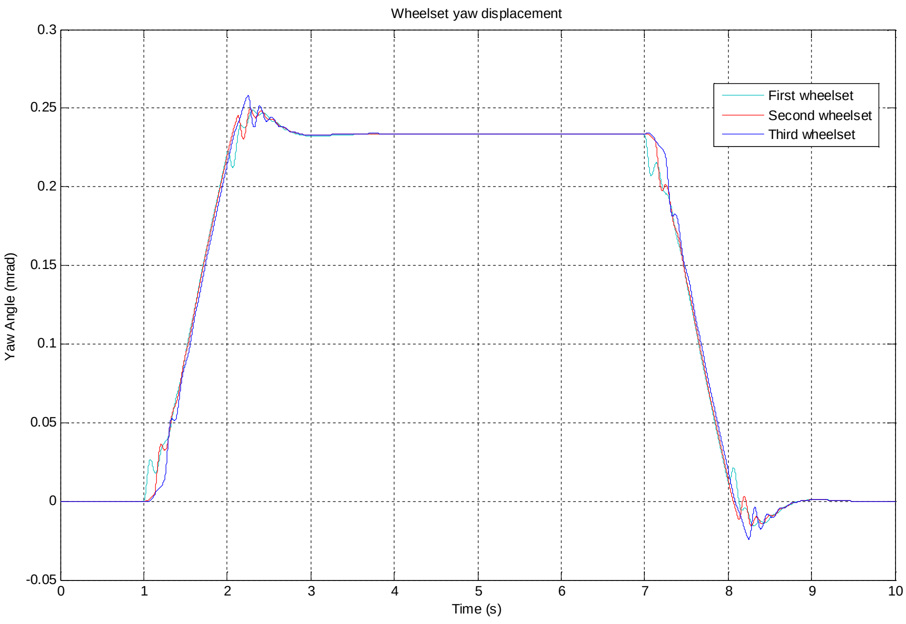

Figure 5.3(e): Yaw angle for parameter curving track radius at 2000 m

Figure 5.4(f) shows the graph of yaw angle result for parameter vehicle velocity value at 80 m/s. The transition states for second and third wheelsets are approximately 0.85 mrad. The transition state for first wheelset is approximately to 0.78 mrad. The steady state for first wheelset is approximately to 0.73 mrad while steady states for second and third wheelset are approximately to 0.79 mrad. Figure 5.4(g) shows the graph of yaw angle result for parameter vehicle velocity value at 100 m/s. The transition states for second and third wheelsets are approximately 1.9 mrad. The transition state for first wheelset is approximately to 1.75 mrad. The steady state for first wheelset is approximately to 1.7 mrad while steady states for second and third wheelset are approximately to 1.8 mrad.

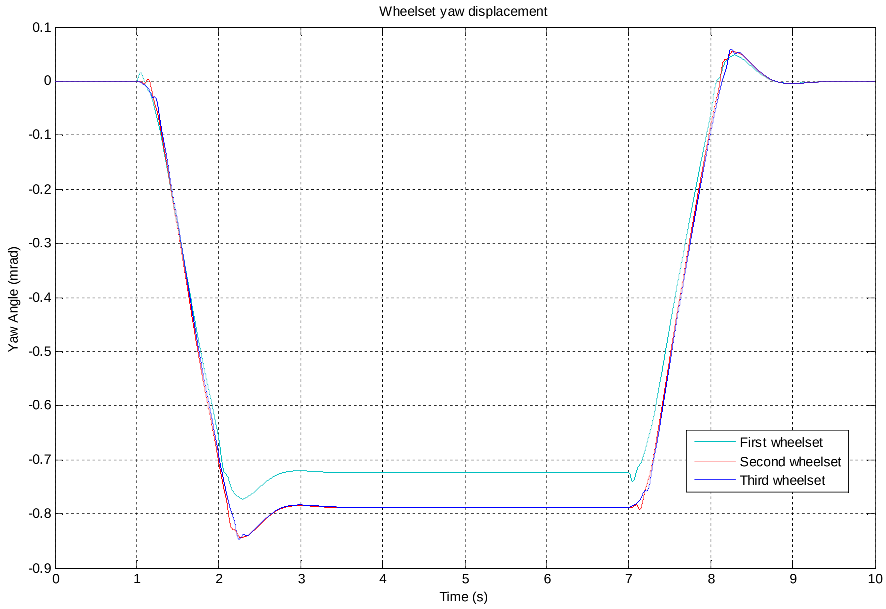

Figure 5.3(f): Yaw angle for parameter vehicle velocity value at 80 m/s

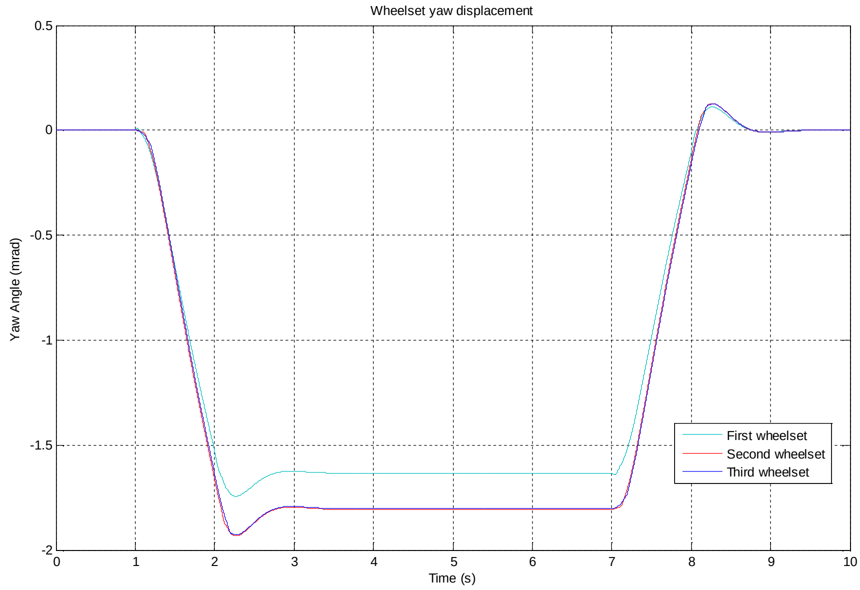

Figure 5.3(g): Yaw angle for parameter vehicle velocity value at 100 m/s

6.3.4 VEHICLE BODY ACCELERATION

Figure 5.4(a) shows the vehicle body acceleration for standard parameter value. The body lateral acceleration on curve transition for three axle vehicle is 0.008 ms^{-2}, as shown in Figure 5.4(a). At steady curve, the lateral acceleration is equal to zero, meaning that no vibration is experienced by the carrying goods during this moment.

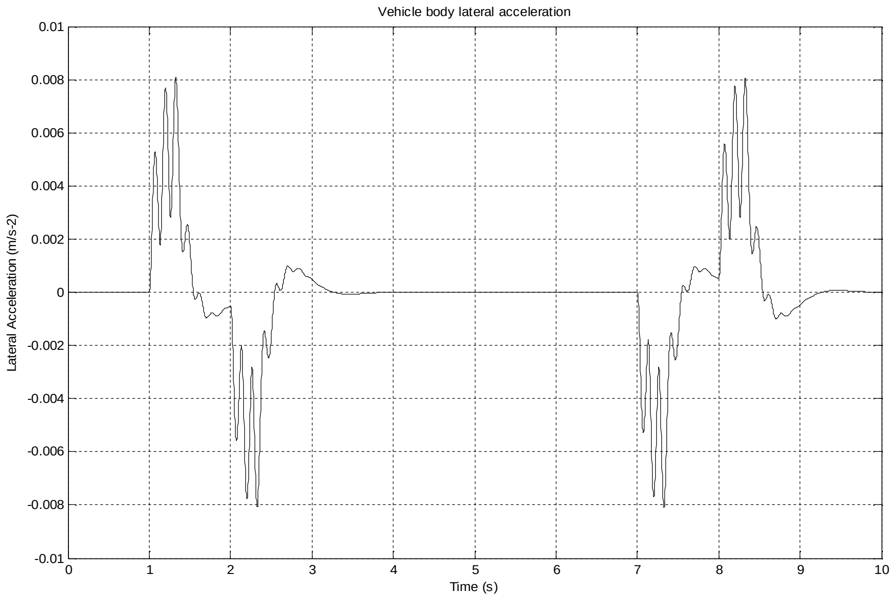

Figure 5.4(a): Vehicle body acceleration for standard parameter value

Figure 5.4(b) shows the vehicle body acceleration for parameter curving track radius value is 1000 m. The body lateral acceleration on curve transition for three axle vehicle is 0.095 ms^{-2}. Figure 5.4(c) shows the vehicle body acceleration for parameter curving track radius value at 2000 m. The body lateral acceleration on curve transition for three axle vehicle is 0.04 ms^{-2}. At steady curve, the lateral acceleration is equal to zero, meaning that no vibration is experienced by the carrying goods during this moment for both graphs.

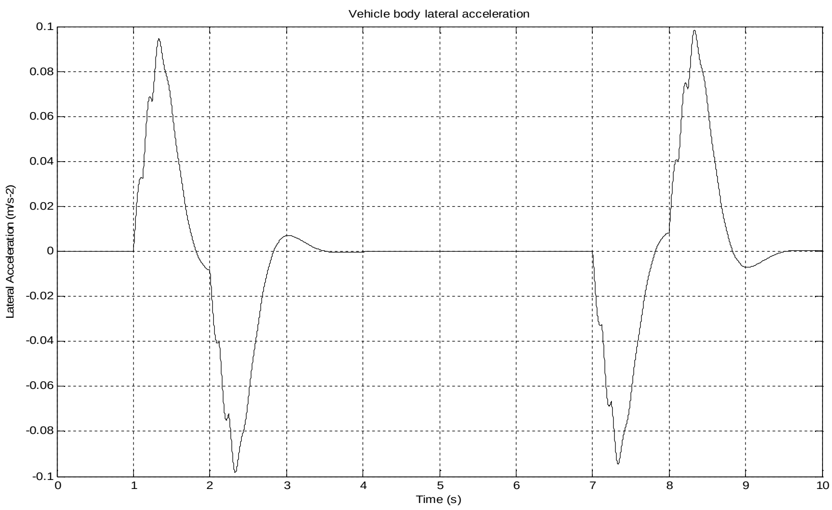

Figure 5.4(b): Vehicle body acceleration for parameter curving track radius at 1000 m

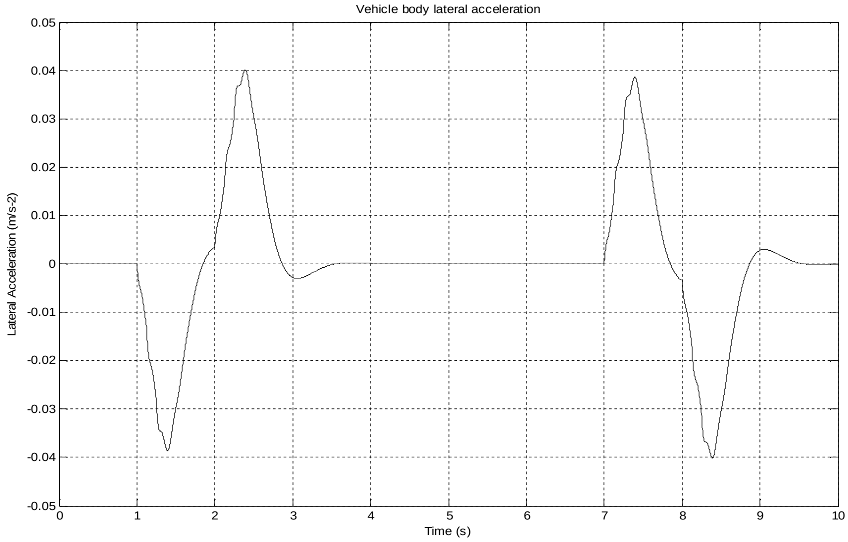

Figure 5.4(c): Vehicle body acceleration for parameter curving track radius at 2000 m

Figure 5.4(d) shows the vehicle body acceleration for cant angle value at 7 degree. The body lateral acceleration on curve transition for three axle vehicle is 0.09 ms^{-2}. Figure 5.4(e) shows the vehicle body acceleration for cant angle value at 21 degree. The body lateral acceleration on curve transition for three axle vehicle is 0.08 ms^{-2}. At steady curve, the lateral acceleration is equal to zero, meaning that no vibration is experienced by the carrying goods during this moment for both graphs.

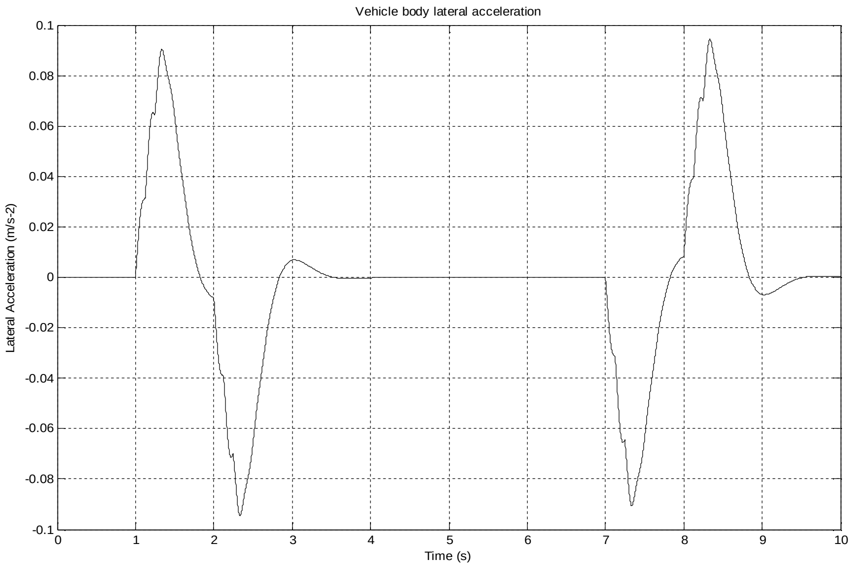

Figure 5.4(d): Vehicle body acceleration for cant angle value at 7 degree

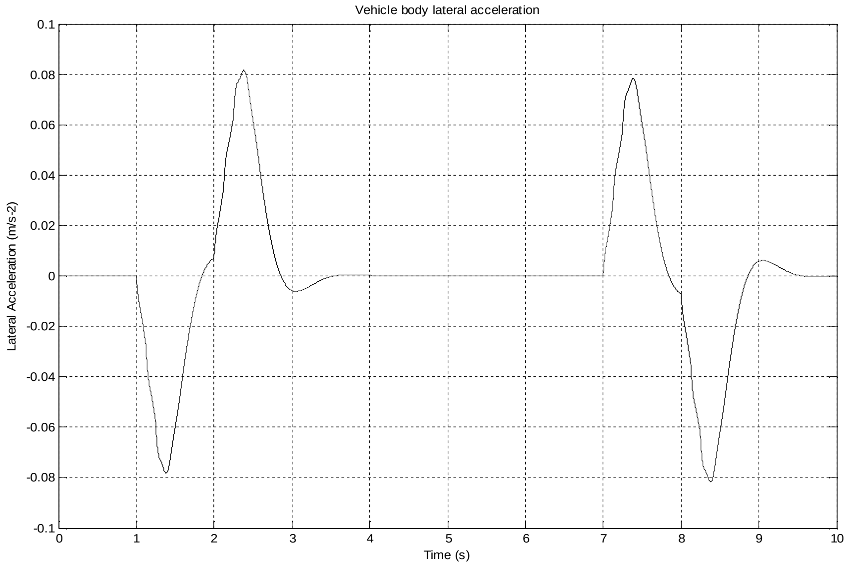

Figure 5.4(e): Vehicle body acceleration for cant angle value at 21 degree

Figure 5.4(f) shows the vehicle body acceleration for parameter vehicle velocity value at 80 m/s. The body lateral acceleration on curve transition for three axle vehicle is 0.15 ms^{-2}. Figure 5.4(g) shows the vehicle body acceleration for parameter vehicle velocity value at 100 m/s. The body lateral acceleration on curve transition for three axle vehicle is 0.35 ms^{-2}. At steady curve, the lateral acceleration is equal to zero, meaning that no vibration is experienced by the carrying goods during this moment for both graphs.

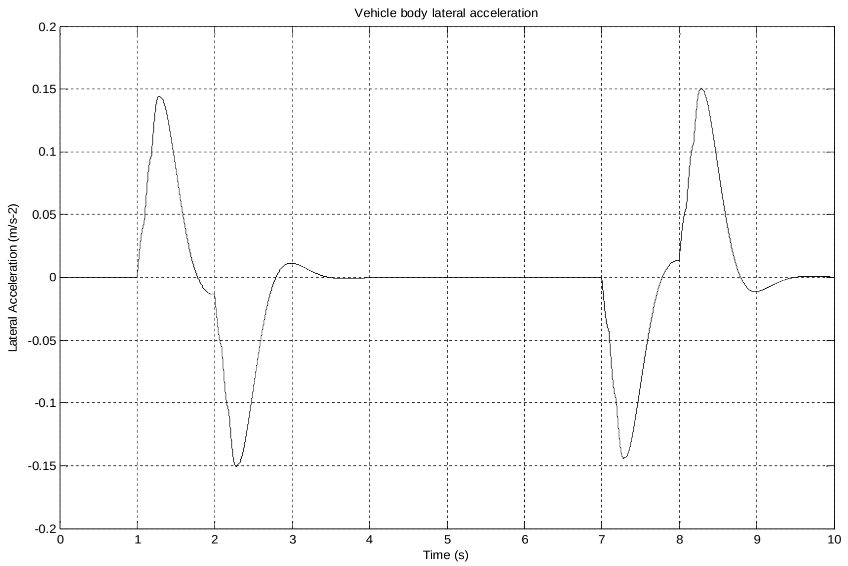

Figure 5.4(f): Vehicle body acceleration for parameter vehicle velocity at 80 m/s

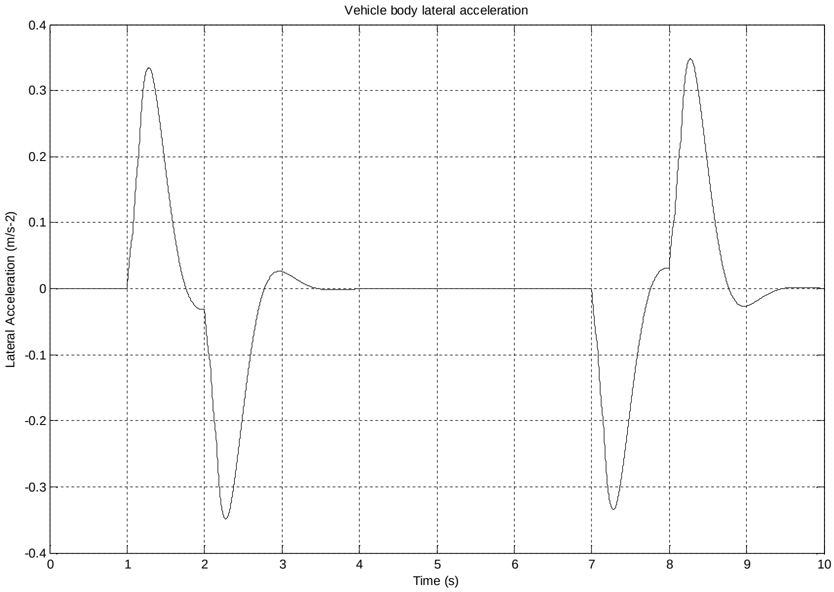

Figure 5.4(g): Vehicle body acceleration for parameter vehicle velocity at 100 m/s

CHAPTER 6

CONCLUSION AND RECOMMENDATIONS

6.1 Conclusion

In the end of this project, the active suspension for three axle railway vehicles has been modelled in state space equation by using MATLAB software. The performance of the train have been analyzed by comparing the result.

After all, the train performance can be improved by applying the active suspension. The best characteristic for cant angle, curving track radius and vehicle velocity can effect the train performance. And the controller selection also one of the important thing to do to get the best result.

6.2 Future Recommendation

For future study or research, there are several improvements can be made to improve the system, there are:

(i) Using different types of modern control technique such as pole placement or SMC

(ii) Study more about the train performance result, which is the effect of third wheelset still not very stable, since when refer to the result graph, the last wheelset does not following the other wheelsets.

REFERENCES

[1] Mohd Anwar b. Zawawi, *Active Suspension System Design for Railway Vehicles Transporting Sensitive Goods and Hazardous Materials*. 2008;4

[2] Kortum, W. and Jaschinski, A. Mechatronic Development for Railway Vehicle of the Future. *Vehicle System Dynamics*. 2000; 9.

[3] Roger Goodall, *Tilting trains and beyond-the future for active railway suspensions (part 2 improving stability and guidance*, COMPUTING & CONTROL ENGINEERING JOURNAL, October 1999, Page 222.

[4] Goodall, R. M. Active Railway Suspensions: Implementation Status and Technological Trends. *Vehicle System Dynamics*. 1997; Vol. 28: 88.

[5] Raman K. Mehra, Jayesh N. Amin, Karl J. Hendrick, Carlos Osario and Srinivasan Gopalasamy, *Active Suspension Using Preview Information and Model Predictive Control*, SBIR Pahse I and US Army, 5-7 October 1997, Page 860 – 861.

[6] T.X Mei, Z. Nagy, R.M Goodall, and A.H *Wickens, Mechatronic solutions for high-speed railway vehicles*, Elsevier Science Ltd., 26 October 2001, Page 1023 – 1028.

[7] Mei, T. X. Perez, J. and Goodall R. M. Design of optimal PI control for perfect curving of railway vehicles with solid-axle wheelsets. *UKACC Int. Conf. on Control 2000*. Cambridge, UK. 2000.

[8] Peterson, G. R. Superelevation and Transition Spiral Primer. 2004. pp. 2.

[9] Rail Safety and Standards Board. Track System Requirement: *Track gauge*. London. Apr. 2007.

[10] Kufver, B. and Forstberg, J. Tracks for Tilting Trains: *Fast and Comfortable Trains*. European Commision. Aug. 2004.

[11] Wikipedia (2009), Linear Quadratic Regulator
URL http://en.wikipedia.org/wiki/Linear-quadratic_regulator

[12] Kalman R.E, 1960 ‘A New Approach to Linear Filtering and Prediction Problems’,*Transactions of the ASME – Journal of Basic Engineering, 82(Series D), pp. 35-45*

[13] William L. Brogan, "Modern control theory", 3rd ed., Englewood Cliffs, N.J., Prentice Hall, 1991

[14] F. L. Lewis (1999). “EE 4343/5329 - Control System Design Project”.

[15] Goodall, R. M. Tilting trains and beyond: The future for active railway suspensions. *Computing & Control Engineering Journal*. Oct 1999; 222.

[16] Mei, T. X. and Goodall, R. M. Optimal control strategies for active steering of railway vehicles. *Proc. IFAC 1999*. Beijing, China. 1999. 215-256.

[17] Goodall, R. M. Tilting trains and beyond: The future for active railway suspensions. *Computing & Control Engineering Journal*. Aug. 1999; 154.

[18] Bryson, A. E. and Ho, Y. C. *Applied Optimal Control*. Waltham, Massachusetts. Blaidshell Publishing Co. 1969.

APPENDIX A: M-FILE FOR ACTIVE SUSPENSION CONTROL OF THREE AXLE RAILWAY VEHICLE MODELING

```
clc;

global A B G uin w;

v=60;
mass=1250;
I=700;
ro=0.45;
length=0.7;
Kl=230e3;
Cl=50e3;

c_1=0.2;
f_1=10e6;


Mb= 13500;
Ib= 170000;
Lb= 3.7;
Lb2=3.7;


B=[0 0 0;
   0 0 0;
   1/I 0 0;
   0 0 0;
   0 0 0;
   0 0 0;
   0 1/I 0;
   0 0 0;
   0 0 0;
   0 0 0;
   0 0 1/I;
   0 0 0;
   0 0 0;
   0 0 0;
   -1/Ib -1/Ib -1/Ib;
   0 0 0];

C_1=[0 1 0 0 0 0 0 0 0 0 0 0 0 0 0 0 ;
    0 0 0 0 0 1 0 0 0 0 0 0 0 0 0 0 ;
    0 0 0 0 0 0 0 0 0 0 1 0 0 0 0 0];

C_yaw=[0 0 0 1 0 0 0 0 0 0 0 0 0 0 0 0 ;
       0 0 0 0 0 0 0 1 0 0 0 0 0 0 0 0 ;
       0 0 0 0 0 0 0 0 0 0 0 1 0 0 0 0];

D=[0 0 0;0 0 0;0 0 0];
```

```
A_1=[-2*f_1/(mass*v)-Cl/mass -Kl/mass 0 2*f_1/mass 0 0 0 0 0 0 0 0
Cl/mass Kl/mass Cl*Lb/mass Kl*Lb/mass ;
     1 0 0 0 0 0 0 0 0 0 0 0 0 0 0 0 ;
     0 -2*f_1*length*c_1/(I*ro) -2*f_1*length^2/(I*v) 0 0 0 0 0 0 0 0 0
0 0 0 0 ;
     0 0 1 0 0 0 0 0 0 0 0 0 0 0 0 0 ;
     0 0 0 0 -2*f_1/(mass*v)-Cl/mass -Kl/mass 0 2*f_1/mass 0 0 0 0
Cl/mass Kl/mass -Cl*Lb/mass -Kl*Lb/mass ;
     0 0 0 0 1 0 0 0 0 0 0 0 0 0 0 0 ;
     0 0 0 0 0 -2*f_1*length*c_1/(I*ro) -2*f_1*length^2/(I*v) 0 0 0 0 0
0 0 0 0 ;
     0 0 0 0 0 0 1 0 0 0 0 0 0 0 0 0 ;
     0 0 0 0 0 0 0 0 -2*f_1/(mass*v)-Cl/mass -Kl/mass 0 2*f_1/mass
Cl/mass Kl/mass -Cl*Lb/mass -Kl*Lb/mass ;
     0 0 0 0 0 0 0 0 1 0 0 0 0 0 0 0 ;
     0 0 0 0 0 0 0 0 0 -2*f_1*length*c_1/(I*ro) -2*f_1*length^2/(I*v) 0
0 0 0 0 ;
     0 0 0 0 0 0 0 0 0 0 1 0 0 0 0 0 ;
     Cl/Mb Kl/Mb 0 0 Cl/Mb Kl/Mb 0 0 Cl/Mb Kl/Mb 0 0 -2*Cl/Mb -2*Kl/Mb
0 0 ;
     0 0 0 0 0 0 0 0 0 0 0 0 1 0 0 0 ;
     Cl*Lb/Ib Kl*Lb/Ib 0 0 -Cl*Lb/Ib -Kl*Lb/Ib 0 0 -Cl*Lb/Ib -Kl*Lb/Ib
0 0 0 0 -2*Cl*Lb^2/Ib -2*Kl*Lb^2/Ib ;
     0 0 0 0 0 0 0 0 0 0 0 0 0 0 1 0 ];

B_ctrl=B(1:16,:);

C_ctrl=[0 1 0 0 0 0 0 0 0 0 0 0 0 0 0 0;
        0 0 0 1 0 0 0 0 0 0 0 0 0 0 0 0;
        0 0 0 0 0 1 0 0 0 0 0 0 0 0 0 0;
        0 0 0 0 0 0 0 1 0 0 0 0 0 0 0 0;
        0 0 0 0 0 0 0 0 0 1 0 0 0 0 0 0;
        0 0 0 0 0 0 0 0 0 0 0 1 0 0 0 0];

D_ctrl=zeros(6,3);
sys1=ss(A_1(1:16,1:16),B_ctrl,C_ctrl,D_ctrl);


Q=diag([100 10 100 10 100 10]*0.001);

R=diag([1e-12 1e-12 1e-12]);


f_sample=400;
sample=1/f_sample;
end_time=10;
end_sim=end_time*f_sample;
t_change=1;
N_recalc=f_sample;
[gain,sol,eigen] = lqry(sys1,Q,R);


g=9.8;
Radius=1500;
```

```
d=14*pi/180;

curve=0;
cant=0;



x0=zeros(16,1);
u0=zeros(3,1);


Ldiff=2*Lb;
t_delay=Ldiff/v;
delay=t_delay*f_sample;
Ldiff2=2*Lb2;
t_delay2=Ldiff2/v;
delay2=t_delay2*f_sample;


s_tran_sec1=1.0;
e_tran_sec1=2.0;
s_tran_sec2=7.0;
e_tran_sec2=8.0;

s_tran1=s_tran_sec1*f_sample;
e_tran1=e_tran_sec1*f_sample;
s_tran2=s_tran_sec2*f_sample;
e_tran2=e_tran_sec2*f_sample;

for i=1:end_sim
    if i>s_tran1 & i<e_tran1
        curve=((1/Radius)/(e_tran1-s_tran1))*(i-s_tran1);
        cant=(d/(e_tran1-s_tran1))*(i-s_tran1);
    elseif i>s_tran2 & i<e_tran2
        curve=((1/Radius)/(s_tran2-e_tran2))*(i-e_tran2);
        cant=(d/(s_tran2-e_tran2))*(i-e_tran2);
    elseif i>=e_tran1 & i<=s_tran2
        curve=1/Radius;
        cant=d;
    else
        curve=0;
        cant=0;
    end
    curve_data(:,i)=[curve(:)];
    cant_data(:,i)=[cant(:)];
end




for t=1:end_sim
   time=(t-1)/f_sample;
```

```
   yt_dot_f= 0 ;
   curve_f=curve_data(t);
   cant_f=cant_data(t);
   t_mid=round(t-delay);
   t_rear=round(t_mid-delay2);

   if t_mid<1
       yt_dot_m=0;
       curve_m=0;
       cant_m=0;
   else
       yt_dot_m=0;
       curve_m=curve_data(t_mid);
       cant_m=cant_data(t_mid);
   end

   if t_rear<1
       yt_dot_r=0;
       curve_r=0;
       cant_r=0;
   else
       yt_dot_r= 0;
       curve_r=curve_data(t_rear);
       cant_r=cant_data(t_rear);
   end


w=[curve_f;cant_f;yt_dot_f;curve_m;cant_m;yt_dot_m;curve_r;cant_r;yt_do
t_r];




   A=[-2*f_1/(mass*v)-Cl/mass -Kl/mass 0 2*f_1/mass 0 0 0 0 0 0 0 0
Cl/mass Kl/mass Cl*Lb/mass Kl*Lb/mass ;
     1 0 0 0 0 0 0 0 0 0 0 0 0 0 0 0 ;
     0 -2*f_1*length*c_1/(I*ro) -2*f_1*length^2/(I*v) 0 0 0 0 0 0 0 0 0
0 0 0 0 ;
     0 0 1 0 0 0 0 0 0 0 0 0 0 0 0 0 ;
     0 0 0 0 -2*f_1/(mass*v)-Cl/mass -Kl/mass 0 2*f_1/mass 0 0 0 0
Cl/mass Kl/mass -Cl*Lb/mass -Kl*Lb/mass ;
     0 0 0 0 1 0 0 0 0 0 0 0 0 0 0 0 ;
     0 0 0 0 0 -2*f_1*length*c_1/(I*ro) -2*f_1*length^2/(I*v) 0 0 0 0 0
0 0 0 0 ;
     0 0 0 0 0 0 1 0 0 0 0 0 0 0 0 0 ;
     0 0 0 0 0 0 0 0 -2*f_1/(mass*v)-Cl/mass -Kl/mass 0 2*f_1/mass
Cl/mass Kl/mass -Cl*Lb/mass -Kl*Lb/mass ;
     0 0 0 0 0 0 0 0 1 0 0 0 0 0 0 0 ;
     0 0 0 0 0 0 0 0 0 -2*f_1*length*c_1/(I*ro) -2*f_1*length^2/(I*v) 0
0 0 0 0 ;
     0 0 0 0 0 0 0 0 0 0 1 0 0 0 0 0 ;
     Cl/Mb Kl/Mb 0 0 Cl/Mb Kl/Mb 0 0 Cl/Mb Kl/Mb 0 0 -2*Cl/Mb -2*Kl/Mb
0 0 ;
```

```
     0 0 0 0 0 0 0 0 0 0 0 0 1 0 0 0 ;
     Cl*Lb/Ib Kl*Lb/Ib 0 0 -Cl*Lb/Ib -Kl*Lb/Ib 0 0 -Cl*Lb/Ib -Kl*Lb/Ib
0 0 0 0 -2*Cl*Lb^2/Ib -2*Kl*Lb^2/Ib ;
     0 0 0 0 0 0 0 0 0 0 0 0 0 0 1 0 ];



   G=[v^2 -g 0 0 0 0 0 0 0;
       0 0 -1 0 0 0 0 0 0;
       2*f_1*length^2/I 0 0 0 0 0 0 0 0;
       0 0 0 0 0 0 0 0 0;
       0 0 0 v^2 -g 0 0 0 0;
       0 0 0 0 0 -1 0 0 0;
       0 0 0 2*f_1*length^2/I 0 0 0 0 0;
       0 0 0 0 0 0 0 0 0;
       0 0 0 0 0 0 v^2 -g 0
       0 0 0 0 0 0 0 0 -1;
       0 0 0 0 0 0 2*f_1*length^2/I 0 0;
       0 0 0 0 0 0 0 0 0;
       v^2/3 -g/3 0 v^2/3 -g/3 0 v^2/3 -g/3 0;
       0 0 -1/3 0 0 -1/3 0 0 -1/3;
       0 0 0 0 0 0 0 0 0;
       0 0 0 0 0 0 0 0 0];


   x=x0;
   uin=u0;
   u(:,t)=[uin(:)];
   [tout,xout]=ode45('train',[time time+sample],x);
   [row,col]=size(xout);
   x0=xout(row,:)';
   xt(:,t)=[x(:)];
   yout=C_1*x0;
   y(:,t)=[yout(:)];
   zout=C_yaw*x0;
   z(:,t)=[zout(:)];



   A_ctrl=[-2*f_1/(mass*v)-Cl/mass -Kl/mass 0 2*f_1/mass 0 0 0 0 0 0 0
0 Cl/mass Kl/mass Cl*Lb/mass Kl*Lb/mass ;
     1 0 0 0 0 0 0 0 0 0 0 0 0 0 0 0 ;
     0 -2*f_1*length*c_1/(I*ro) -2*f_1*length^2/(I*v) 0 0 0 0 0 0 0 0 0
0 0 0 0 ;
     0 0 1 0 0 0 0 0 0 0 0 0 0 0 0 0 ;
     0 0 0 0 -2*f_1/(mass*v)-Cl/mass -Kl/mass 0 2*f_1/mass 0 0 0 0
Cl/mass Kl/mass -Cl*Lb/mass -Kl*Lb/mass ;
     0 0 0 0 1 0 0 0 0 0 0 0 0 0 0 0 ;
     0 0 0 0 0 -2*f_1*length*c_1/(I*ro) -2*f_1*length^2/(I*v) 0 0 0 0 0
0 0 0 0 ;
     0 0 0 0 0 0 1 0 0 0 0 0 0 0 0 0 ;
     0 0 0 0 0 0 0 0 -2*f_1/(mass*v)-Cl/mass -Kl/mass 0 2*f_1/mass
Cl/mass Kl/mass Cl*Lb/mass Kl*Lb/mass ;
     0 0 0 0 0 0 0 0 1 0 0 0 0 0 0 0 ;
```

```
     0 0 0 0 0 0 0 0 0 0 -2*f_1*length*c_1/(I*ro) -2*f_1*length^2/(I*v) 0
0 0 0 0 ;
     0 0 0 0 0 0 0 0 0 0 1 0 0 0 0 0 ;
     Cl/Mb Kl/Mb 0 0 Cl/Mb Kl/Mb 0 0 Cl/Mb Kl/Mb 0 0 -2*Cl/Mb -2*Kl/Mb
0 0 ;
     0 0 0 0 0 0 0 0 0 0 0 0 0 1 0 0 0 ;
     Cl*Lb/Ib Kl*Lb/Ib 0 0 -Cl*Lb/Ib -Kl*Lb/Ib 0 0 Cl*Lb/Ib Kl*Lb/Ib 0
0 0 0 -2*Cl*Lb^2/Ib -2*Kl*Lb^2/Ib ;
     0 0 0 0 0 0 0 0 0 0 0 0 0 0 1 0 ];


   sys=ss(A_ctrl(1:16,1:16),B_ctrl,C_ctrl,D_ctrl);

       [gain,sol,eigen] = lqry(sys,Q,R);
       u0=-gain*x0(1:16);

   u_data(:,t)=[u0(:)];

   gain_data(:,t)=[gain(:)];

   acc(:,t)=A(13,:)*x0(:)+B(13,:)*u0(:)+G(13,:)*w(:);

end



%%%%%%%%%%%%%%%%%%%%%%%%%%%%%%%%%%
%%%%%%% PERFORMANCE PLOTS %%%%%%%
%%%%%%%%%%%%%%%%%%%%%%%%%%%%%%%%%%
p=sample:sample:end_time;

figure(1)
subplot(2,1,1);
plot(p,curve_data,'k');
ylabel('1/Radius (1/meter)');
xlabel('Time (s)');
grid;
title('Curve')
subplot(2,1,2);
%figure(2)
plot(p,cant_data/pi*180,'k');
ylabel('Cant angle (degree)');
xlabel('Time (s)');
grid;
title('Cant');

figure(3)
plot(p,u_data,'k');
ylabel('Control Torque (Nm)');
xlabel('Time (s)');
grid;
title('Control torque');

figure(4)
```

```
plot(p,y*1e3,'k');
ylabel('Lateral Displacement (mm)');
xlabel('Time (s)');
grid;
title('Wheelset lateral displacement');

figure(5)
plot(p,z*1e3,'k');
ylabel('Yaw Angle (mrad)');
xlabel('Time (s)');
grid;
title('Wheelset yaw displacement');

figure(6)
plot(p,acc,'k');
ylabel('Lateral Acceleration (m/s-2)');
xlabel('Time (s)');
grid;
title('Vehicle Body Lateral Acceleration');
```